MULTI-BASELINE POLINSAR INVERSION AND SIMULATION OF INTERFEROMETRIC WAVENUMBER FOR FOREST HEIGHT RETRIEVAL USING SPACEBORNE SAR DATA

KRISHNAKALI GHOSH
March, 2018

SUPERVISORS:
Mr. Shashi Kumar
Dr. Valentyn A. Tolpekin

MULTI-BASELINE POLINSAR INVERSION AND SIMULATION OF INTERFEROMETRIC WAVENUMBER FOR FOREST HEIGHT RETRIEVAL USING SPACE-BORNE SAR DATA

KRISHNAKALI GHOSH
Enschede, The Netherlands, [March, 2018]

Thesis submitted to the Faculty of Geo-Information Science and Earth Observation of the University of Twente in partial fulfilment of the requirements for the degree of Master of Science in Geo-information Science and Earth Observation.
Specialization: Geoinformatics

SUPERVISORS:
Mr. Shashi Kumar, IIRS
Dr. Valentyn A. Tolpekin, ITC

THESIS ASSESSMENT BOARD:
Dr.Ir. R.A. de By (Chair)
Prof. Dr. Ir. A. Stein (ITC Professor)
Dr. Anup Das (External Examiner, Space Application Centre (SAC), Ahmedabad)

"There is always something more to learn."
-Master Oogway

ABSTRACT

Maintenance of a global forest inventory and regular monitoring of forests is necessary to assess the global carbon stock. Forests have versatile functionality for the mankind and the demands could be fulfilled only by judicious assessment of forest biophysical parameters. Forest height is a parameter essential for quantitative monitoring of forests. Remote sensing tools can efficiently monitor forests on a global scale. Many studies have attempted to use Synthetic Aperture Radar (SAR) remote sensing to estimate forest parameters. This research explores Polarimetric SAR Interferometry (PolInSAR), a technology well suited for forest height estimation. The focus of this work is the retrieval of tree heights in Barkot and Thano forests of India using multi-baseline X-band data while attempting to optimize the estimation performance by simulation of wavenumber. Coherence amplitude inversion and three-stage inversion are performed to estimate the tree heights. Previous studies have used datasets with baseline information suitable for height estimation. This research attempts to use datasets with inapt baseline information and imitates the ideal wavenumber condition. The wavenumber is calculated based on the prior knowledge of the maximum tree height in the region of study. The tree height estimates obtained from both inversions are validated against field data. The accuracy of tree height estimates increase from 24.91% to 88.28% when the ideal wavenumber is used. The minimum calculated RMSE is 1.46m for three-stage inversion and 1.96m for coherence amplitude inversion. The results suggest that using an optimal wavenumber can improve the tree height estimation process.

Keywords: coherence, coherence amplitude inversion, three-stage inversion, optimization, wavenumber, baseline

ACKNOWLEDGEMENTS

I wish to take this opportunity to thank the two most important people for their contributions throughout the duration of this research, my supervisors. I am grateful to Mr. S. Kumar for his patient supervision and motivation and Dr. V.A. Tolpekin for his consistent encouragement and valuable feedback. While the dream of achieving something very extraordinary was short-lived, I am thankful to my supervisors for pulling me through the days of uncertainty. I sincerely appreciate them for the mentorship and help they have extended at every step. Their guidance has helped me grow immensely as a researcher and I will treasure all the advices proffered.

Thanks to all the staff at Indian Institute of Remote Sensing and Faculty of Geo-Information Science and Earth Observation, ITC- University of Twente for they played a considerable part during this tenure. Especially, I express my gratitude to Dr. A. Senthil Kumar (Director, IIRS) for providing all the opportunities and facilities. Special thanks to Dr. Sameer Saran (HOD-GID, IIRS) for his concern and encouragement.

In addition, I wish to thank my classmates at IIRS and ITC for sticking together through both good and trying times. I appreciate the affability of my PG Diploma, ITEC and CSSTEAP friends who helped maintain the optimism all along.

Lastly, I extend heartfelt appreciation to my family for the constant moral support and affection. They have always been my inspiration, and I dedicate this to them. Like Calvin once said "I must obey the inscrutable exhortations of my soul." thank you for always motivating me to follow my desires.

TABLE OF CONTENTS

LIST OF FIGURES

LIST OF TABLES

1. INTRODUCTION

The terrestrial biosphere (soil, vegetation) and oceans are the major carbon sinks where atmospheric carbon gets sequestered. Changing carbon content in the atmosphere gradually affects the carbon cycle and climate due to the greenhouse effect. Assessing the forest biomass is important for monitoring the quantity of carbon that is impacted by deforestation, and estimation of carbon stock in a forest ecosystem (Vashum & Jayakumar, 2012). Forest height is a noteworthy parameter to consider for assessment of the carbon reserve. Information about forest height is important to carbon stock estimation and classification of vegetation types. It is also necessary to determine the weather impact, diseases in vegetation and unlawful cutting of trees. It has been reported that deforestation practices have vastly contributed to global climate change (Dixon et al., 1994). These reasons make research on retrieval of forest height information quite essential.

Remote sensing provides information from a vast area over a regular interval of time thus, making it beneficial over field survey. To monitor large forest areas remotely sensed information from different satellites can be deemed useful. Advancements in the remote sensing techniques and geoinformation systems have helped researchers to study forest canopy, height, basal area, and diameter. Radar remote sensing is advantageous over other types of remote sensing due to its capability to acquire data irrespective of climatic condition. In active radar remote sensing, information is gained from the backscatter received from microwaves transmitted by satellite. The use of longer wavelength microwaves in radar remote sensing allows penetration through cloud cover. This property makes radar remote sensing efficient for the study of forest parameters as it can penetrate through dense canopy. Moreover, longer wavelength allows low atmospheric scattering which makes detection of microwave energy possible at any time of the day.

Synthetic aperture radar (SAR) uses the forward motion of the radar to create a synthetic aperture. It takes into account the Doppler Effect for simulation of a large synthetic antenna. As the radar passes a given target, pulses are reflected in sequence. These reflected signals are combined to generate an aperture which provides a higher resolution than real aperture radar systems. Many researchers have previously applied SAR remote sensing data to study above ground biomass and have found it to contain inadequate information. For forests, scattering is considered from the top of the canopy, forest ground and tree branches and trunks. Different species of trees show different scattering patterns owing to their height, leaf area, and canopy structure. Research on advanced methods for SAR signal processing can help in better understanding of the forest structure.

Polarimetric SAR (PolSAR), Interferometric SAR (InSAR) and Polarimetric Interferometric SAR (PolInSAR) techniques were developed to enhance the application of radar remote sensing. Radar polarimetry is a unique technique to extract geophysical information from SAR data. It works with signals with different transmitted and received polarizations. The polarimetric radar can operate as single polarization, dual polarization or quadratic polarization system which means that single polarized transmitted waveform can return a single polarized (horizontal or vertical), dual polarized (HV and HH) or quadratic polarized (HH, HV, VH, and VV) signal. Various polarimetric combinations are used to extract meaningful information about the target surface. Additionally, interferometry considers interferograms formed by the capture of signals from different phases and different angles. This is based on a coherent combination of two or more complex SAR images. Interferometry varies with topography, structure, and density of the scattering target.

PolInSAR combines the benefits of polarimetry and interferometry. Polarimetry effectively explains the scattering patterns from targets and interferometry explains the phase difference and position of the target. In PolInSAR a change in polarization leads to change in the phase of the interferogram. The difference between the initial and new phase of the interferogram is strongly correlated to actual forest height. Scattering by vegetation in PolInSAR data results in low coherence where interferometry permits adjusting coherence via changing baselines. Forest height retrieval algorithms using PolInSAR data have been previously studied (Cloude & Papathanassiou, 1998; Mette et al., 2004). PolInSAR has been observed to overcome the limitations of PolSAR and InSAR. This can lead to a notable improvement in the quality of forest height estimation. A quadratic polarization radar system is used for transmitting signals and receiving information in two orthogonal polarizations which create a scattering matrix leading to polarization signature generation. The polarization signatures observed from the scattering target depend on the type of scattering, surface, double-bounce or volume. There is significant processing improvement in quadratic polarization PolInSAR data over single polarization data for forest height estimation (Cloude & Papathanassiou, 1998).

Vertical wavenumber (k_z) is calculated based on baseline, wavelength, angular separation of acquisitions and the angle of incidence. k_z scales the relation of interferometric phase and coherence factors to forest height. A change in k_z corresponds to change in coherence at a given height (Kugler et al., 2015). Since estimation process depends on the coherence, it is indirectly impacted by the k_z value used. Single value of k_z results in inversion of only limited range of tree heights. Use of large k_z result in underestimation of larger heights whereas, small k_z result in coherence to forest height scaling errors (Kugler et al., 2015). For improved accuracy in forest height inversion k_z should lie within a suitable range. This forms the basis for formulation of PolInSAR inversion models. Depending on the forest height multiple wavenumbers could be considered to validate the inversion model.

Forest height inversion algorithms using k_z consider baseline value as an important input parameter. The baseline value should be such that the height of ambiguity (or the height corresponding to interferometric phase change) is more than the maximum forest height in the given area. Larger baseline shows low ambiguity in height whereas smaller baseline show better sensitivity interferometer (Krieger et al., 2010). Spaceborne SAR systems provide data with smaller baselines and larger height of ambiguity which makes study of multiple baselines necessary for ideal forest height estimation. The incidence angle is another important parameter for k_z calculation. The local incidence angle changes for different terrain slopes which is responsible for different values of k_z. For a decrease in incidence angle volume coherence decreases and vice versa. Thus, precise estimation of k_z can be done while making use of terrain information from digital elevation models like digital surface model.

Simulation is the replication of an ideal scenario to understand a system. Simulations are usually performed for optimization of a model. While working with multiple baseline PolInSAR, there may be interferometric pairs with a very large height of ambiguity which would require wavenumber simulation to achieve an appropriate height of ambiguity. Inversion performance can be impacted by simulation of vertical wavenumber to generate an improved model. For realizing exact height estimates temporal decorrelation should be minimal and multiple baselines should be available. Research to establish the effect of simulated wavenumbers on PolInSAR inversion models is limited.

Spaceborne SAR data effectively covers a larger area than airborne SAR which makes it useful for the wider expanse of forested areas. Previously many researchers have studied the volume structure of forests using spaceborne PolInSAR data (Treuhaft & Siqueira, 2000; Krieger et al., 2005; Perko et al, 2011). Acquisition of multiple sensor data can enhance the tree height retrieval. Unlike repeat-pass sensors which have the larger time difference between each pass, TerraSAR-X and TanDEM-X fly in a single-pass bistatic mode with a formation such that there is no effect of temporal decorrelation and do not show atmospheric or scene changes. Estimation of vegetation height from interferometric measurements of bands like X-band depends on the coherence and phase. Multiple baselines, spatial or temporal are used for model parameterizations. Distinctive wavenumbers from multi-baseline data can be used to estimate interferometric parameters at different polarizations (Neumann et al., 2010). Long baselines and higher coherence yield vegetation height with fewer errors. But spaceborne SAR has smaller baseline resulting in higher errors and low volume decorrelation (Krieger et al., 2005). Simulation of wavenumbers will help indicate ideal baselines such that the inversion models can provide forest height estimation with reduced errors.

For extraction of vegetation parameters, inversion of scattering models is crucial. Some of the common inversions for forest parameter retrieval are coherence amplitude inversion (Cloude, 2005), three-stage inversion (Cloude & Papathanassiou, 2003) and Random Volume over Ground (RVoG) model (Cloude & Papathanassiou, 2001). Coherence amplitude inversion considers low surface to volume scattering ratio while considering only amplitude and ignoring the coherence phase. Three-stage inversion considers cross polarized channel for height estimation. Previously, it proved efficient for undulating terrains with forested slopes (Cloude & Papathanassiou, 2003). Whereas RVoG considers two layer scattering, that is, from ground and canopy. The topography is assumed as a flat plane for calculation of the coherence and volume correlation which leads to an estimation of height. In reality, the ground topography is undulating which should be considered for height estimation and to achieve precision inversion algorithms must be incorporated in RVoG model. Along with this, temporal decorrelation needs to be considered for multiple pass data acquisition. Longer baseline with changes of ground and volume scattering pattern affects the temporal decorrelation. It is a task to account for the temporal decorrelation to optimize the evaluation of inversion.

Temporal decorrelation biases in space-borne SAR make an estimation of forest height with high accuracy, a challenge. However, the single-pass TerraSAR-X and TanDEM-X combination avoids this bias thus, making it useful for PolInSAR applications. Due to a large area covered by a PolInSAR imagery, consideration should be given to different vegetation species variety which has different scattering pattern and spectral signatures. The effect of vertical wavenumber on inversion should be focused to understand the inversion performance. Therefore, the main objective of this study would be to simulate the wavenumber for optimum inversion performance in forested areas.

1.1. Problem Statement

PolInSAR inversion is based on the sensitivity of phase and coherence to the vertical components like leaves and branches and sensitivity of polarimetry to the orientation of these vertical components. Previous studies have mainly used inversion models for forest height estimation on airborne SAR data. The limitation of using airborne SAR data is that it is susceptible to imaging geometry problems due to a wider range of incidence angle unlike space-borne SAR data, which have narrow incidence angle (15º-60º for TerraSAR-X StripMap mode), wider swath and uniform revisits that makes it more suitable for useful applications. However, airborne SAR systems can collect data at desired look angle and direction. This flexibility has made airborne SAR systems more convenient for the development of the forest height inversion algorithms (Cloude, 2005). The challenge with using space-borne PolInSAR data is that to achieve optimized coherence; low height of ambiguity and large baseline should be used.

For vegetation study, smaller baselines provide higher coherence (Sagués et al., 2000). Coherence is proportional to the phase difference between the interferogram which can infer low noise in the image pairs. So, for forest parameter retrieval high coherence pattern is essential. Smaller baselines would result in the higher height of ambiguity that would impact the forest height estimation. The previous studies have suggested that vegetation provides low coherence which limits its utility for forest height estimation. Interferometry individually is ambiguous at areas of higher forest density due to interferograms generated by other physical factors (Treuhaft & Siqueira, 2000). Evaluation of the tree height above ground necessitates the information of vertical profiles which can be estimated from the use of multiple baseline data.

This study will consider SAR quadratic polarized data with multiple baselines for maximum information gain. Using quadratic polarized dataset and different inversion models, this research will aim to identify the backscatter from forest canopy while considering optimization of the accuracy of forest height estimation. To improve the coherence, multi-baseline interferometric pairs would consider the simulation of wavenumbers to acquire suitable height of ambiguity. Additionally, the study would explore the impact of wavenumbers on the PolInSAR inversion models.

1.2. Research Identification

1.2.1. Research Objective

Prime focus of the present work is to apply model inversion to retrieve forest height from multi-baseline X-band polarimetric SAR interferometry (PolInSAR) data and to evaluate the potential of interferometric vertical wavenumber in model output.

1.2.2. Sub-objectives

1. To generate suitable interferometric vertical wavenumber for interferometric pairs using simulation approach based on minimum object height and SAR geometrical parameters.
2. To implement the three-stage inversion and coherence amplitude inversion for forest height retrieval.
3. To evaluate the potential of simulated vertical wavenumber in forest height retrieval as compared to height retrieval from SAR geometry.
4. To assess accuracy and validate modeled output using field data

1.2.3. Research Questions

1. How does the information of SAR geometry influence the vertical wavenumber?
2. How can tree height be estimated from the observed complex coherence?
3. What is the effect of different inversion modeling approaches on the estimated tree height?
4. Is there a difference in the height estimated from simulated wavenumber and SAR geometry?
5. How accurately do the modeled output relate to the available field data?

1.3. Innovation aimed at

The novelty of this research is to improvise on PolInSAR inversion models using simulated wavenumber for forest height retrieval.

2. LITERATURE REVIEW

Synthetic Aperture Radar (SAR) systems operate with virtual aperture antennas which offer high spatial resolution radar images. The SAR images acquired from airborne or spaceborne platforms are useful in extraction of information and analysis. Varied operational wavelengths of SAR systems are appropriate for different applications. For the study of forest parameters previously various bands (L, C, P, X etc.) have been used. The longer wavelength corresponds to deeper penetration through canopy thus, L and P band show major scattering from tree trunks whereas X and C bands show major scattering from top of canopy. Advanced remote sensing techniques such as Polarimetric SAR Interferometry (PolInSAR) have been utilized for forest height and biomass estimation (Cloude & Papathanassiou, 2003; Cloude et al., 2013; Tong et al., 2016).The penetration capability is low at X band but studies have shown the potential of parameter inversion from TerraSAR-X and TanDEM-X data (Kugler et al., 2014).

2.1. Polarimetric SAR Interferometry

First demonstrated in 1998 on spaceborne Imaging Radar mission (SIR-C/X) data, PolInSAR is a procedure to study the combination of polarimetric scattering from an interferometric pair of dataset. Forests display complex scattering of signals which can be interpreted using PolInSAR (Hellmann & Cloude, 2007). Researchers have studied the applications of PolInSAR using single baseline (Cloude & Papathanassiou, 2001) and multi-baseline data (Neumann et al., 2010). PolInSAR combines pairs of polarimetric images using interferometry to acquire information. In SAR remote sensing a scattering matrix [S] contains the pixel-wise information of amplitude and phase of the signals. The scattering matrix can be written as a vector using Pauli basis and lexicographic basis (Cloude & Pottier, 1996). Pauli basis can be used to represent different scattering mechanisms like $S_{HH}+S_{VV}$ for surface scattering, $S_{HH}-S_{VV}$ for double bounce scattering and $S_{HV}+S_{VH}$ for volume scattering. Two SAR sensors separated by spatial baseline (B) obtain images (s_1 and s_2) of an area, which are used to acquire three dimensional information. Information related to height can be obtained from SAR images acquired at different incidence angles ($\theta_1$and θ_2). A detailed PolInSAR geometry is shown in Figure 1.

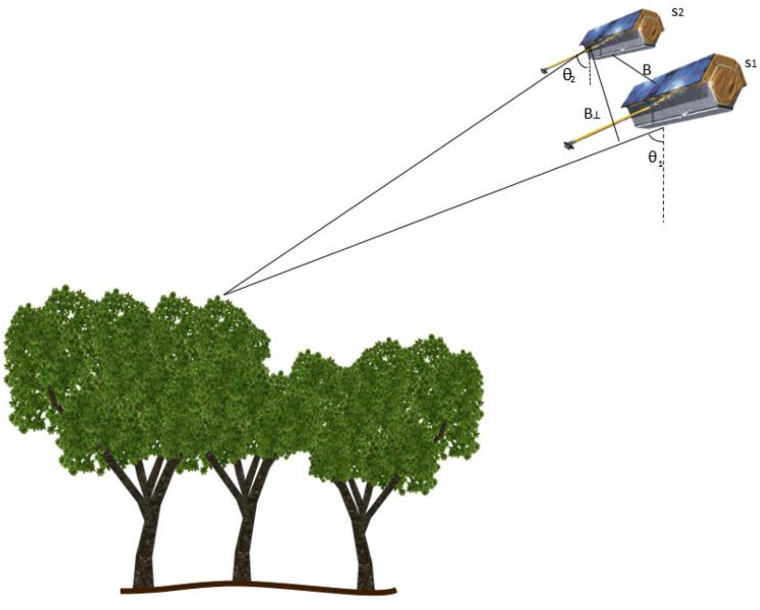

Figure 1. Representation of PolInSAR geometry with TerraSAR-X and TanDEM-X satellites separated by a spatial baseline B acquiring images s_1 and s_2. The effective perpendicular baseline is denoted by $B_\perp$ and the angle of incidence is denoted by $\theta_1$and θ_2 where $\theta_2=\theta_1+\Delta\theta$. (Not to scale.)

The phase of SAR signals linearly depend on the slant range distance and the scatterers. The difference in phase of acquisitions and projection of flat ground topography on radar geometry determines the scattering phase centre (Lee, 2012). Description on the basics of SAR is presented in Appendix 1.

2.1.1. Phase to height interpretation

The elementary targets can be distributed in the form of surface or volume structures. The complex forms like forests show multiple scattering from the likes of leaves, twigs, branches and stem. Forest canopy is majorly volume scatterers that can be modelled as random cloud of scatterers for which topographic phase determine the height sensitivity of interferometric phase. The height of a scatterer within a resolution cell can be derived from the system geometry and phase information. The acquisition of interferometric pairs with change in incidence angle is reflected by a change in the phase of the propagating signals. The phase and height relationship is established with consideration of a local coordinate system around the scatterer where the axes determine the interferometric phase. The dependence of the phase on the surface position in the local coordinate system is eliminated to relate phase to only height. The factor that relates phase to height is implemented as a scaling factor. Wavenumber, in general, is the spatial frequency of a wave and it represents the scaling factor in interferometry. For spaceborne systems with very large range as compared to spatial baseline, the change in incidence angle can be approximated as the effective perpendicular baseline times range inverse. The difference in geometry of PolInSAR acquisitions form a parameter called interferometric wavenumber (k_z) (Kugler et al., 2015). k_z represents wavenumber in the direction of height and measures the height sensitivity in PolInSAR inversions. The unit of k_z is radm^{-1} and is given as:

$$k_z = m\frac{2\pi}{\lambda}\frac{B_\perp}{R\sin\theta} \tag{1}$$

m can be 1 or 2 depending on acquisition mode, R is the range and $B_\perp$ corresponds to effective perpendicular baseline which is the projection of spatial baseline on the range. The height sensitivity of an interferometric pair can be determined from the ratio of baseline to wavelength. The Equation (1) suggests that increasing the baseline improves the sensitivity of system to height. But it holds true only till certain baseline length (called the critical baseline) after which the area overlap in the interferometric pair reduces thus impacting the resolution. Critical baseline is the baseline after which correlation between the image pair becomes zero (Cloude, 2010). TerraSAR-X exhibits critical baseline within few kilometres for the incidence angles ranging between 20 to 50 degrees (Krieger et al., 2010).

The interferometric phase can be related to terrain height by interferometric wavenumber as:

$$h_{\mathcal{Topo}} = \frac{\varphi_{\mathcal{Topo}}}{k_z} \tag{2}$$

The height that leads to 2π phase change is called height of ambiguity (Ferrettiet al., 2007). A small height of ambiguity corresponds to a small change in phase. It provides a better understanding of elevation and is given as:

$$\mathcal{HoA} = \frac{2\pi}{k_z} \tag{3}$$

From (1) and (3) it can be established that the baseline is inversely proportional to height of ambiguity which determines the sensitivity of PolInSAR to height differences. Forestry applications use height of ambiguity larger than the tree height for estimation process (Sagués et al., 2000).

2.1.2. PolInSAR coherence

Coherence is the cross correlation of two SAR images from different acquisitions. The complex coherence accounts for both interferometric phase and interferometric coherence. When two acquisitions are done from different positions two different scattering matrices are produced. The scattering matrices are used to generate a 6×6 Hermitian positive semi definitive matrix [T_6]. The T_{11} and T_{22} are 3×3 matrices Hermitian coherency matrices containing information about polarimetric properties and Ω_{12}, also a 3×3 matrix contains polarimetric and interferometric information both. For two images s_1 and s_2 of the same area from different incidence angles and polarizations represented by unitary vectors ($\vec{\omega}_1, \vec{\omega}_2$) for both images (Cloude & Papathanassiou, 1998) complex interferometric coherence can be given as:

$$\tilde{\gamma} = \frac{\langle \overrightarrow{\omega_1}^{\dagger} [\Omega_{12}] \vec{\omega}_2 \rangle}{\sqrt{\langle \vec{\omega}_1^{\dagger} [T_{11}] \vec{\omega}_1 \rangle \cdot \langle \overrightarrow{\omega_2^{\dagger}} [T_{22}] \vec{\omega}_2 \rangle}} \tag{4}$$

Where ⟨…⟩ represents the expected value applied for averaging. The range of values for modulus of amplitude of coherence can be from no correlation at 0 to full correlation at 1 for the pair of SAR images. In a SAR image the resolution cell can contain information from distributed scatterers which may give inaccurate coherence and phase information which can be handled by dividing the image using number of looks. The number of looks influences the level of coherence and is necessary for the estimation of accuracy for the measured coherence values (Touzi et al., 1999; Bamler & Hartl, 1998).

2.1.2.1. Decorrelation

Decorrelation can be defined as the process which reduces the correlation between the two acquired image pairs. The coherence depends on two types of parameters, acquisition parameters and structural parameters of scatterers. The observed coherence includes the contribution from different processes causing decorrelation (Krieger et al., 2005; Bamler & Hartl, 1998). Forestry applications take into consideration three kinds of decorrelation: system, scattering and temporal (Zebker & Villasenor, 1992; Lee, 2012). System decorrelation considers majorly the effect of two components: noise due to non-ideal SAR systems (signal to noise ratio) and processing. Noise is usually due to unstable system and sensors. Noise contributions in the two consecutive signals of an interferometric acquisition are not correlated. The signal to noise ratio decorrelation can be defined as the ratio of scattering power to received power. The signal to noise ratio decorrelation at different polarizations influences the coherence (Hajnsek et al., 2001). Another component of system decorrelation is co-registration decorrelation which depends on the accuracy of co-registration which is governed by level of coherence (Chen et al., 2016). Scattering decorrelation considers the effect of two components: spectral decorrelation and volume decorrelation (Kugler et al., 2015). The change in the incidence angle for acquisition corresponds to a change in range and azimuth which influences the ground wavenumber spectra and is responsible for spectral decorrelation (Gatelli et al., 1994). The spectral information from one image is observed in the other image with a slight shift in the spectrum which depends on the topographical condition, incidence angle, wavelength and baseline. It contains information of a three dimensional scene in a two dimensional geometry. The different scattering processes at different heights in a pixel are responsible for volume decorrelation. The vertical scattering information in two images are projected differently thus inducing a loss in coherence (Treuhaft & Siqueira, 2000). Temporal decorrelation considers the effect of changes in geometry or dielectric properties of scatterers that occurred between the time intervals of two acquisitions. Small temporal baselines corresponds to decorrelation due to wind induced motion in forests. It is very difficult to predict and model temporal decorrelation, however, many models and effects of temporal decorrelation have been studied over years (Zebker & Villasenor, 1992; Lee et al., 2009).

2.1.3. Coherence optimization

In PolInSAR selection of scattering mechanism by combination of polarimetric channels can be used for interferometric processing. Coherence optimization is an approach to evaluate the polarization for obtaining highest coherence (Cloude & Papathanassiou, 1998). The higher value of coherence corresponds to better estimation of phase, thus, making coherence optimization important for PolInSAR applications. Coherence information from different polarizations represent predominance of different scattering mechanisms. For example, cross polarization (HV) is considered to have dominant volume scattering information. For forestry applications estimating canopy height, the idea is to select two coherence with maximum interferometric phase separation to distinctly identify topographic phase from the top of canopy phase. To serve the purpose of optimization the [T_6] matrix containing the polarimetric and interferometric information is calculated. The major assumptions for modelling of coherence are no change in polarimetric characteristics of scatterers between two acquisitions (i.e. $T_{11} \approx T_{22}$) which hold true for small temporal baselines and equivalent projection vectors for both acquisitions (Neumann et al., 2008; Lavalle, 2009). This assumption characterizes the optimization to be phase sensitive thus leading to an approach of separation in coherence.

2.1.4. Fundamentals of coherence region

Interferometric coherence is dependent on polarization and all possible coherence values for different polarizations can be geometrically represented by points in a unit circle. The range of the coherence values depicted by these points together is called the coherence region as shown in Figure 2 (Flynn et al., 2002; Cloude, 2010). The coherence region is useful for the depiction of both amplitude and phase optimization to identify two scattering mechanisms with maximum interferometric coherence separation. The shape and size of coherence region depends on the scattering process, system noise, number of looks and radar geometry (Cloude, 2010).

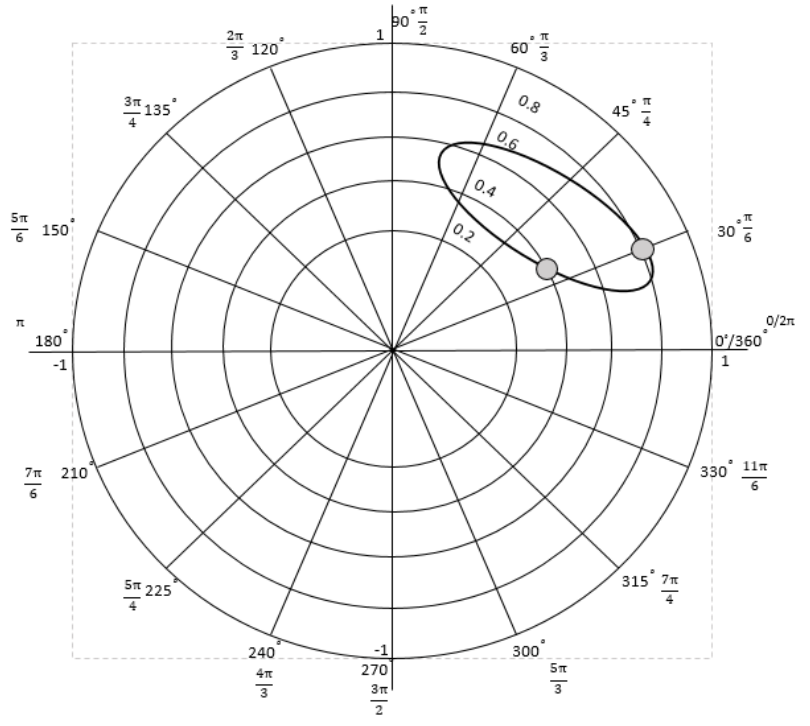

Figure 2. Unit circle showing the Coherence region for a PolInSAR matrix where the angle denote the phase information and the coherence region denote the variation in amplitude of coherence.

For different polarizations, the range of interferometric coherence can be indicated from the angular extent of coherence in the unit circle. The varying value of phase (φ) from 0 to π alters the boundary of the coherence region. The polarimetric diversity information from the coherence region has been studied to differentiate crop types from X-band data (Krieger et al., 2013). X-band does not penetrate to greater depths in dense forests thus there is less variations observed than data acquired with longer wavelength for different backscatters in coherence region.

2.2. Models for forest height estimation

Various models have been developed to replicate forest structure and study the height of forests. Training course on PolInSAR (Cloude, 2005) demonstrates many forest height estimation techniques using these models. Scientists have established forward and inverse models (Le Toan et al., 1992; Ranson et al., 1997; Cloude & Papathanassiou, 2003) for forest backscatter. Forward modeling estimates the SAR return as a function of wave parameters, like polarization, frequency, incidence angle, geometry and properties of the forest. Inversion models use the SAR return datasets to estimate forest properties. Forest backscatter models are broadly divided into three types: physical, empirical and semi empirical. Physical models are based on the scattering behavior of target object and electromagnetic theory. Empirical models are based on fitting of mathematical equation to experimental data like regression. These models are computationally efficient and represent backscatter information in a simplified approach. Semi-empirical models are based on both scattering behavior and empirically established equation. These models exploit the advantageous features of both empirical and physical models (van Der Sanden, 1997) by providing easier inversion and high accuracy in estimation. Forest height estimation algorithms have been studied using coherence information, decomposition patterns and tomography (Neumann et al., 2010; Kumar et al., 2017; Fu et al., 2017; Tebaldini, 2012). Research on comparative analysis of different forest height estimation algorithms have shown significant variations in estimation results (Zhou et al., 2013; Joshi et al., 2016).

2.2.1. Inversion methods

Sensitivity of PolInSAR system to vertical structure and material properties of scatterers have made it valuable for forest parameter extraction. While using a scattering model with certain parameters and observations the inverse of model provides the estimate of the parameters. Least squares study is undertaken to reduce the difference between the parameters and their estimation. There are many inversion strategies as discussed.

2.2.1.1. Inversion using phase difference

To invert a model the phase should be estimated. The phase with maximum surface scattering is identified for the purpose. Using the volume coherence the phase for different polarizations can be acquired. DEM differencing method (Cloude & Papathanassiou, 1998) calculated the difference between pure surface scattering and pure volume scattering to determine the forest height. Zhang et al., in 2017 studied this method with cross polarization channel HV to find complex coherence from volume scattering and co polarization HH-VV to find complex coherence from surface scattering. This method resulted in underestimation of forest height. Since the phase center for cross polarization channel can lie between top of canopy and center of tree height the estimation depends on the structure of the forest and its density. Many algorithms for phase optimization (Yamada et al., 2001), coherence optimization (Flynn et al., 2002) have been studied over years. Optimization algorithms are based on selection of polarizations with maximal phase difference to estimate forest heights.

2.2.1.2. Inversion using physical models

Physical models describe the structure of the forest beneficial for estimation of the height. Models consider trees as cylindrical scatterers for simplified analysis. Random Volume over Ground (RVoG) is a commonly used two layer scattering model which considers vegetation and ground as the scattering layers (Cloude & Papathanassiou, 2003). RVoG considers a randomly oriented volume of height h_v over a ground positioned at $z=z_0$. The interferometric coherence from the volume scatterers depends on the response from scatterers at different heights within the medium. It also depends on the extinction of radar wave within the medium. Both the vertical structure of forest and the extinction can be proposed to influence the forest height estimation. Across the range of frequencies of X band to P band the RV assumption have been proven valid for experimental datasets (Hajnsek et al., 2009). Two inversion methods coherence amplitude inversion and three-stage inversion are based on the physical model.

Coherence Amplitude Inversion

The volume decorrelation increases with the increased vegetation density which corresponds to reduced coherence. Coherence amplitude inversion is a technique based on this phenomenon. Two polarization channels predominantly with volume scattering and with surface scattering are selected and the coherence amplitude is studied to estimate the volume. This inversion is sensitive to the density of forest which corresponds to a change in the extinction value and the structure of the canopy which corresponds to the phase. This makes it necessary for consideration of both phase and coherence for strong estimation, which have been studied by various algorithms (Joshi et al., 2016).

Three-Stage Inversion

The implementation of PolInSAR model for forest height using polarization independent coherence is presented by the three-stage inversion process (Cloude & Papathanassiou, 2003). The technique calculates complex coherence for different polarizations in three stages by fitting of least square lines, followed by removal of vegetation bias and estimation of extinction. Inversion of the complex coherence uses two variable phases to find a straight line which best fits the coherence region inside a unit circle. For estimation least square fit helps in providing the minimum error solution while minimizing the uncertainties. It considers the coherences that are more distant from maximum phase difference. The vegetation bias is calculated by estimating the ground topographic phase. Ground topography is estimated from the coherence and ground to volume scattering ratio. The high ground to volume scattering ratio values is used to identify the true ground phase. The ground to volume scattering is more for higher value of coherence i.e. near to the boundary of the unit circle. When minimum ground to volume scattering ratio is zero it corresponds to volume only coherence but higher values necessitate consideration of extinction information. The dissimilar extinctions for different scattering medium restricts the inversion algorithm performance (Hajnsek et al., 2009). The height and extinction variation is analysed to find the coherence loci for volume coherence. The minimum non negative ground to volume scattering ratio helps to determine the solution for height estimation. The three-stage inversion considers that there is one polarization channel with pure volume scattering, which could not be possible due to different penetration depths which have been administered in recent researches (Lin et al., 2017).

2.2.2. Impact of wavenumber

For solving the forest height inversion the information of vertical wavenumber (k_z) is crucial. Wavenumber relates interferometric phase to the height of scatterers. Impact of k_z on the forest height inversion using PolInSAR data has been explored by researchers for various SAR wavelength data. It has been observed that only a certain range of k_z values correspond to correct inversion for a given range of tree heights. For a too large values of k_z the coherence saturates at certain forest height and for a too small values of k_z the coherence cannot segregate the forest heights (Kugler et al., 2015). The range of k_z should be selected so as to optimize the inversion procedure while taking into consideration the extinction value and the ground topology. The coherence to height and phase to height comparison is shown in Figure 3. Performance of the inversion procedure depends on the choice of suitable wavenumber. An increase in the vertical wavenumber for a certain forest height results in decrease in coherence levels. The coherence is sensitive to the forest height up to a certain tree height range after which there are underestimations as can be seen from Figure 3 where the 50 m (red) and 40 m (yellow) showing low coherence for larger k_z values. For the optimization of $k_{z,}$ a number of diverse baselines should be analysed. The terrain information in range direction influences the local incidence angle which is necessary for accurate estimation of tree heights (Kugler et al., 2015).

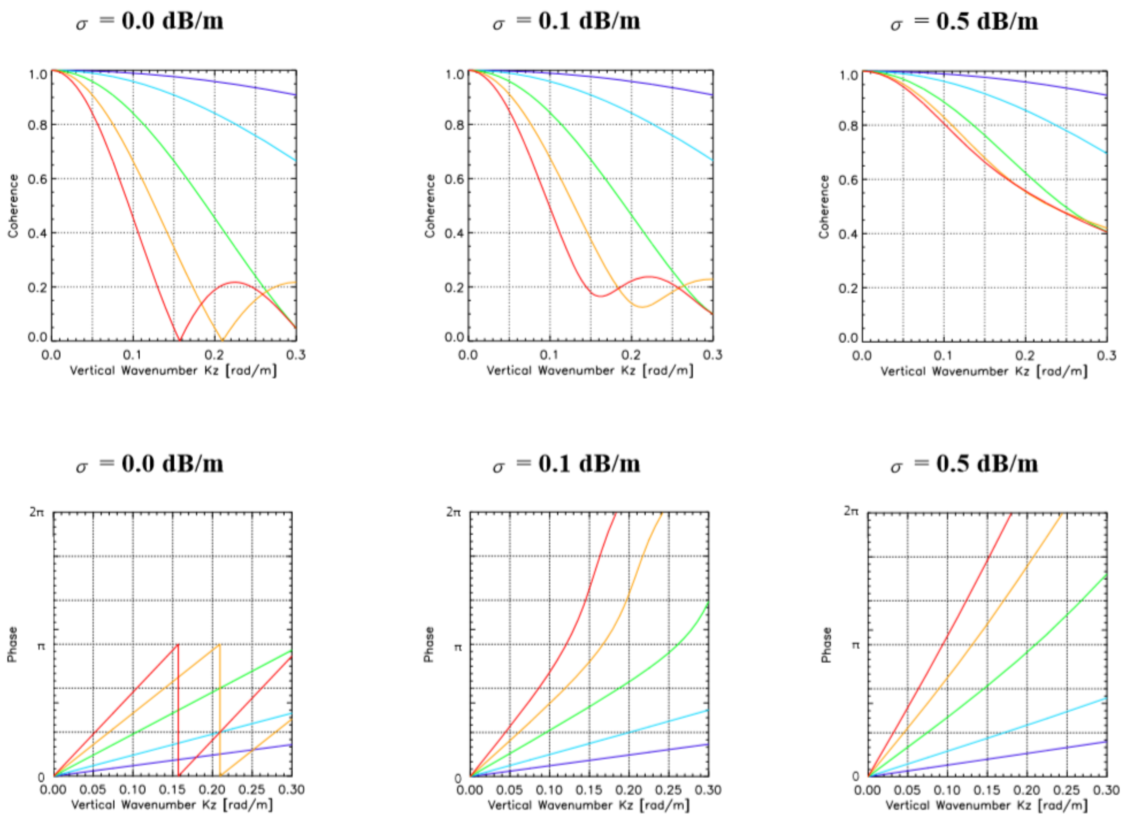

Figure 3. Plots showing dependence of coherence and phase on vertical wavenumber for three extinctions of 0dB/m, 0.1dB/m and 0.5dB/m (Source: Kugler et al., 2015)

2.3. High frequency data for forest height estimation

High frequency X-band data provides good height estimation results in sparse forest (Praks et al., 2009). The performance of X-band for forest height estimation depends on the canopy density and dielectric properties which are highly influenced by seasonal variations. The impact of polarization on the coherence also influences the capability of information retrieval. Since X band does not penetrate deep into dense forest its accuracy to retrieve forest height is still being explored. Studies focussing on the PolInSAR data for both airborne and spaceborne sensors have been done (Lopez-Sanchez et al., 2017; Perko et al., 2011; Cloude et al., 2013). This research aims to explore the capability of X band data from TerraSAR-X and TanDEM-X to estimate forest height while taking into consideration the influence of vertical wavenumbers.

3. METHODOLOGY

This research work majorly concentrates on estimation of forest height using PolInSAR data acquired by X-band spaceborne sensor while taking into consideration the impact of changing vertical wavenumber on the estimation accuracy. The following methodology is adopted to achieve the objective of this project:

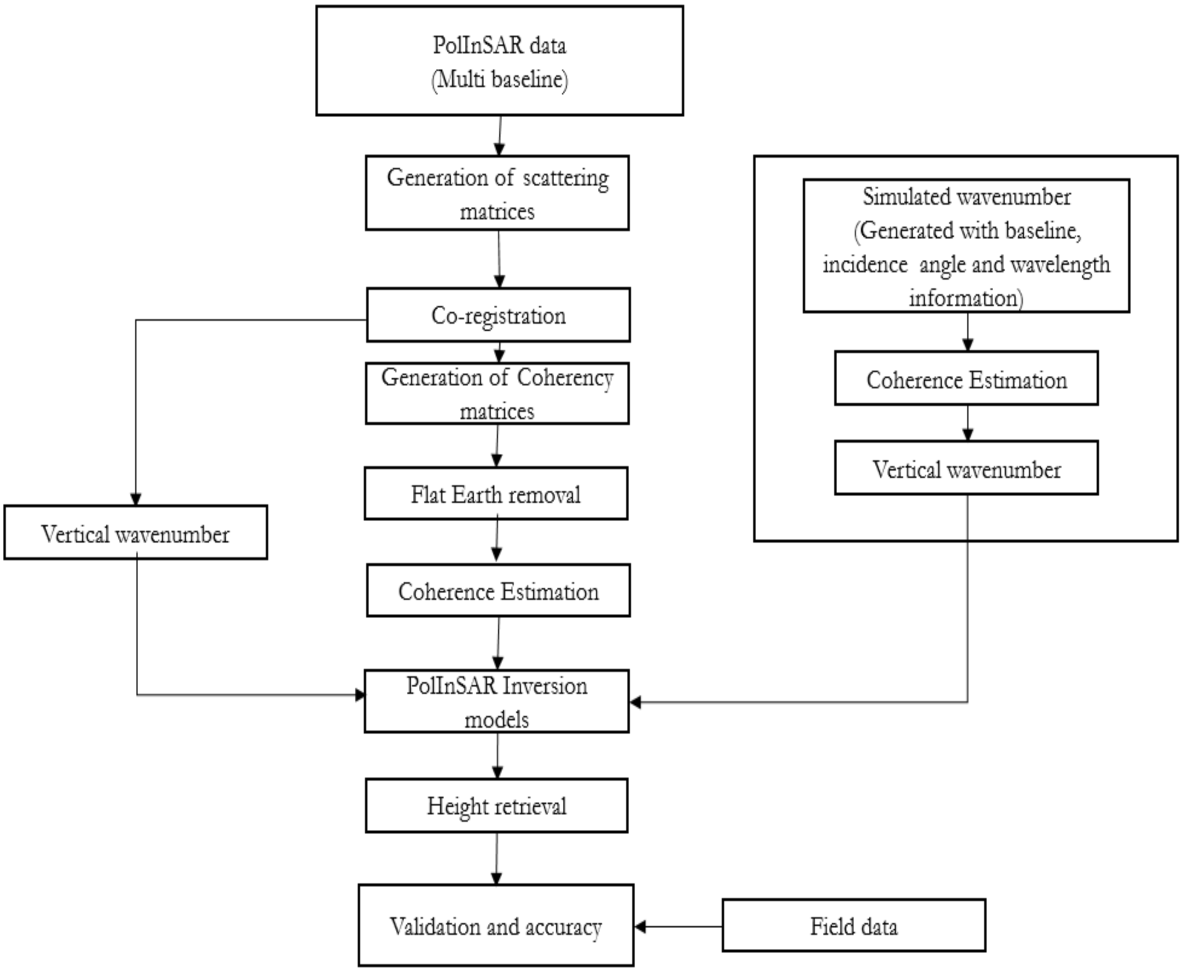

Figure 4. Methodology for PolInSAR processing

3.1. PolInSAR data processing

The PolInSAR data processing takes into account two acquisitions of the same area from different location and time. For this study TerraSAR-X and TanDEM-X acquisitions with varied spatial and temporal baselines are used. Absolute radiometric calibration considers both the backscatter and the radar brightness and minimizes the difference between the radiometry of acquisitions done on different geometry. Level 1 SAR products which have radiometric bias need radiometric calibration prior to any quantitative analysis. The data is calibrated for pixel values to represent the true backscatter. The complex outputs after calibration are stored to acquire useful information of both phase and amplitude for forest height estimation. These complex output are used to calculate the DN values in the images.

3.1.1. Scattering matrix generation

The radar system transmits and receives signals of either same or different polarizations owing to the target properties. The scattering from the target varies with the frequency and wavelength, incidence angle, look direction and polarization of radar system. It also varies with the surface roughness, slope, orientation angle and dielectric constant of the target. The scattering matrix stores the values from the different polarization channels. The scattering matrix for all the datasets are generated to obtain the backscatter information. The 2×2 matrices of dataset are used for analysis as a pair of master and slave with scattering matrix [S_1] and [S_2], respectively in the horizontal-vertical basis as:

$$[S_1] = \begin{bmatrix} S_{HH}^1 & S_{HV}^1 \\ S_{VH}^1 & S_{VV}^1 \end{bmatrix} \tag{5}$$

$$[S_2] = \begin{bmatrix} S_{HH}^2 & S_{HV}^2 \\ S_{VH}^2 & S_{VV}^2 \end{bmatrix} \tag{6}$$

3.1.2. Co-registration

Co-registration aligns images to provide backscatter information from same ground position while minimizing the loss in coherence. It applies spectral analysis on the scattering matrices of master and slave images. The process of co-registration is necessary for determination of difference in phase between acquisitions depending on spatial and temporal baselines. The acquired data are collocated centred on reference geometry of master image thus, the images have same size and geo-positioning.

3.1.3. Wavenumber computation

Vertical wavenumber relates the phase information to the height of scatterer and is calculated using the Equation (1). The difference between the incidence angles for two acquisitions which is related to the perpendicular baseline information in case of spaceborne systems is used for this study. The wavenumber changes with the incidence angle which is dependent on the terrain slope. For positive slope, value of k_z is more than for negative slope. The height estimation uses $k_z$as a scaling factor. SAR geometry calculation is used to find the suitable range of k_z and later ideal values can be simulated for the estimation of tree height.

3.1.4. Coherency and covariance matrix generation

To acquire scattering information from multiple targets within a pixel (also, distributed scatterer) coherency matrix and covariance matrix are generated. The information from only the scattering matrix is insufficient to explain the backscatter from multiple scatterers. The coherency matrix is generated from the scattering matrix using a scattering vector for monostatic system (Cloude & Pottier, 1996) as:

$$k_L = [S_{HH} \quad \sqrt{2}S_{HV} \quad S_{VV}]^T \tag{7}$$

$$k_P = \frac{1}{\sqrt{2}}[S_{HH} + S_{VV} \quad S_{HH} - S_{VV} \quad S_{HV} + S_{VH}]^T \tag{8}$$

The vectors k_L and k_P denote the lexicographic and the Pauli basis, respectively. The superscript ^{T} denotes transpose of a matrix, the first term of subscript denotes the received signal polarization and the second term denotes the transmitted signal polarization.

The Pauli basis can be used to explain the different scattering mechanisms. The association between different polarization images is calculated using the covariance matrix [C_3] and coherency matrix [T_3] given as:

$$[C_3] = \langle k_L k_L^{\dagger} \rangle \tag{9}$$

$$[T_3] = \langle k_P k_P^{\dagger} \rangle \tag{10}$$

Where † denotes the complex conjugate transpose and ⟨⟩ denotes the spatial average. The spatial averaging is used for the assumption of a homogenous scattering medium. In PolInSAR, coherency matrix of two images of same area are used for generation of a 6×6 complex coherence matrix [T_6]. The elements in the complex coherence matrix store both polarimetric and interferometric information. For two images with scattering matrices [S_1] and [S_2] and Pauli basis scattering vectors k_1 and k_2 the coherence matrix [T_6] is given as (Cloude & Papathanassiou, 1998):

$$[T_6] = \langle \begin{bmatrix} k_1 \\ k_2 \end{bmatrix} [k_1^{\dagger} \quad k_2^{\dagger}] \rangle = \begin{bmatrix} [T_{11}] & [\Omega_{12}] \\ [\Omega_{12}^{\dagger}] & [T_{22}] \end{bmatrix} \tag{11}$$

3.1.5. Interferogram generation

The interferogram comprises information from the ground and the canopy layer. It is generated to obtain information about topography in an area. It is the complex conjugate of the images s_1 and s_2, as mentioned in Section 2.1. The phase of a pixel contains two parts, one dependent on the distance of target from sensor and another on the property of scatterer called scattering phase. The interferogram shows the variation in phase for two interferometric acquisitions given as:

$$\varphi_i = \frac{-4\pi}{\lambda} r_i + \varphi_{s_i} \quad \text{i} = 1,2 \tag{12}$$

Where r is the range distance, $\varphi_1$is the phase of master image, φ_2 is the phase of slave image and λ is the wavelength. Due to minute difference in the look angle for spaceborne datasets, the scattering phases can be considered equal. Thus, the interferogram depends on the difference in the range distance of acquisitions only. The interferometric phase is composed of phase differences due to topology, flat earth, forest height, noise and atmospheric changes.

3.1.6. Flat earth removal

For analysis of a pair of interferometric images it is necessary to find the phase difference related to height of the object. The phase difference observed from two points with same terrain height and different range distance is called the flat earth phase. The flat earth phase is eliminated from the interferometric phase to obtain the phase difference caused by forest height. The variation in the phase for the flat earth is removed by multiplying the interferogram with the complex conjugate of flat earth phase (Cloude, 2005). So after the phase variation from the flat ground is removed the interferometric phase only relates to the forest height.

3.1.7. Coherence estimation

Complex coherence is used to calculate the correlation between an interferometric pair. As discussed in Sub-section 2.1.2, complex coherence is obtained by vectorization of the interferometric coherence. The amplitude of the complex coherence ranges from 0 to 1. When complex coherence is 0 there is no noteworthy correlation between the pixels of both images and when 1 there is total correlation. The coherence amplitude image is a greyscale image which does not contain information about the phase. For this reason coherence is represented in a unit circle which can help visualise coherence and phase value for each pixel individually. In this study the complex coherence is calculated for linear (HH, HV, VH, VV), circular (LL, LR, RR), Pauli (HH+VV, HV+VH, HH-VV) and optimal basis (Opt1, Opt2, Opt3) calculated from coherence maximization in different polarization states. Mathematical transformation can be used to obtain polarization matrix of different basis. For different polarization basis the coherence value changes. The complex coherence for all basis are used to estimate height of trees using three-stage inversion in the study area. The amplitude of coherence varies with the property of scatterer and the polarization. The forested areas usually are expected to show low coherence values due to high volume decorrelation. The constraint with coherence complex plane is that it is not capable to show the variation in coherence of each pixel altogether.

3.1.8. Height estimation from inversion

For the estimation of height of forests in a study area the coherence amplitude and coherence phase information is used. The coherence amplitude inversion model which relates height to coherence amplitude at zero extinction follows a sinc curve (Cloude, 2005). This relationship is implemented to estimate forest height values for coherence in a particular channel. The polarization channel HV+VH has very low surface to volume scattering ratio that results in low coherence value. The phase information is ignored and coherence is compared to the random volume prediction to achieve height estimates. For study of forested areas the random volume is considered with no effect from polarization. The surface scattering and random volume scattering information is used in PolInSAR processing through the random-volume-over ground model approach (Cloude & Papathanassiou, 2003). The coherence values should be different so as to maximise stability of inversion process.

3.1.8.1. Coherence Amplitude Inversion

Coherence amplitude inversion is centred on the idea that coherence is inversely related to the density of volume in a forested area. It calculates the difference between the coherence from top phase layer and ground phase layer. The coherence which shows predominantly surface scattering is considered as purely ground phase and the coherence which shows volume scattering is considered as top phase. In this inversion method only the amplitude value of coherence is used while neglecting the phase information. The coherence amplitude gives the height estimate as a solution of the equation:

$$F = \left\| \left| \widetilde{\gamma_{\omega_v}} \right| - \left| \frac{p}{p_1} \frac{e^{p_1 h_v} - 1}{e^{p h_v} - 1} \right| \right\| \tag{12}$$

Where F is a function which has to be minimized, $\|..\|$ denotes Euclidean norm vector, $\tilde{\gamma}$ stands for observed volume coherence, h_v is the vegetation layer height, $\bar{\sigma}$ stands for mean extinction, $p = \frac{2\bar{\sigma}}{\cos\theta}$ and $p_1 = p + ik_z$. $\min_{h_v} F$ takes values equal to and greater than zero.

3.1.8.2. Three-Stage Inversion

Based on the RVoG model as discussed in Subsection 2.2.1, three-stage inversion is developed on the two layers vegetation model. This model considers that the canopy extends from the ground to top. It calculates the complex coherence as a combination of polarization independent volume integral (γ_v) and polarization dependent ground to volume scattering ratio$\mu(\omega)$.

$$\mu(\omega) = \frac{2\sigma}{\cos\theta_0\left(e^{\frac{2\sigma h_v}{\cos\theta_0}} - 1\right)} \frac{\omega^\dagger T_g \omega}{\omega^\dagger T_v \omega} \tag{13}$$

$$\gamma_v = \frac{2\sigma}{\cos\theta_0\left(e^{\frac{2\sigma h_v}{\cos\theta_0}} - 1\right)} \int_0^{h_v} e^{ik_z z'} e^{\frac{2\sigma z'}{\cos\theta_0}} dz' \tag{14}$$

The polarization dependent complex coherence can be depicted as a straight line in a complex plane as:

$$\gamma(\omega) = e^{i\phi_1}\left(\gamma_v + L(\omega)(1-\gamma_v)\right) \qquad 0 \le L(\omega) \le 1 \tag{15}$$

$$L(\omega) = \frac{\mu(\omega)}{1+\mu(\omega)} \tag{16}$$

Where σ is the mean extinction, h_v is the vegetation layer height, T_v and T_g are the volume scattering and ground scattering coherency 3×3 diagonal matrices. The three-stage inversion model utilizes the coherence optimization for finding the maximum and minimum ground component scattering ratio. Representation of the solution of (15) on the unit circle help in identification of the ground only phase. The solution line intersects the circle at two points one being the true solution and another false (which is rejected by inversion process). At one point on the line $\mu = 0$ which is considered as the position of volume coherenceγ_v. The visible length of the solution line is dependent on the SAR geometry and vegetation density. It is used for the inversion which is a three stage procedure.

From the plot of coherences on complex plane as shown in Figure 17 the best fit line is first plotted using the total least square line fit. Linear coherences (HH, HV, and VV) and Pauli coherences (HH+VV, HH-VV and HV+VH) sometimes due to variations in coherence and phase do not give a good line fit for which Optimum coherences (Opt1, Opt2, and Opt3) may be used. Coherence optimization identifies the highest coherence values while minimizing variations. Phase diversity (PD) coherences with maximum and minimum phase differences can be used for coherence optimization. One of the intersection points among ψ_1 and ψ_2 of the best fit line with the complex plane is considered for estimation of volume only coherence. The polarizations are ranked with respect to the ground to volume scattering ratio and the one intersection point farthest from the lowest is considered to provide correct estimate for ground topography. The function of volume coherence can be depicted in the complex plane for different extinctions to establish a relation between coherence and vegetation layer height. The intersection of curve from this function and best fit line are used to findμ. From these the negative values of μ are rejected. This is used to estimate the coherence and eventually reach at the estimated height of vegetation.

3.2. Simulation of wavenumber

Tree height estimates should tend towards the true value for a dataset with optimal baseline. To achieve accurate tree height estimate the perpendicular baseline should be such that sensitivity to height is maximal and observed ambiguity is minimum. The height estimation of volume scatterers depends on the coherence. From Equation (2) the interferometric height is scaled by the wavenumber. For a true surface topography:

$$h_v = \frac{\arg(\gamma_v e^{-i\phi})}{k_z} \Rightarrow h_v = \frac{\mathcal{H}\sigma\mathcal{A}}{2\pi}\left[\arg\left(\gamma_v e^{-i\phi}\right)\right] \tag{17}$$

$\mathcal{H}\sigma\mathcal{A}$ is an indicator for h_v and ϕ is estimated from the available datasets. Coherence optimization is taken into consideration to improve the estimation process while scaling h_v by using$\mathcal{H}\sigma\mathcal{A}$. The direct proportionality of perpendicular baseline and k_z from Equation (1) dictates the height sensitivity.

The height sensitivity of an InSAR pair depends on the ratio$\frac{B}{\lambda}$. From Subsection 2.1.1, as the baseline approaches critical baseline the correlation between InSAR pair reduces. For accurate tree height estimation an appropriate baseline would have $\mathcal{H}\sigma\mathcal{A} > \max(h_v)$ (Kugler et al., 2014). Additionally, the ideal $\mathcal{H}\sigma\mathcal{A}$

should be around two times the maximum tree height in the given area (Olesk et al., 2016; Chen et al., 2016). This evaluates the acceptable value of $k_z \geq 0.09$.

To achieve the desirable range of k_z for correct tree height estimates, from Equation (1), a perpendicular baseline should be predicted while keeping the values of λ, $\sin\theta$ and R as constant. The range of k_z computed from the predicted baseline must be implemented in the tree height estimation. The inverse proportionality of $\mathcal{H}\sigma\mathcal{A}$ with $B_\perp$ is the underlying notion for the height retrieval using the virtually computed k_z. A prior knowledge of tallest tree height from field data is necessary to calculate ideal range of k_z. For mature Sal forests like Barkot forest the maximum tree height is approximately 30 m. From the SAR geometry and predicted $B_\perp$, the range of $0.1 \leq k_z \leq 0.21$. The following methodology is used for optimization of inversion performance:

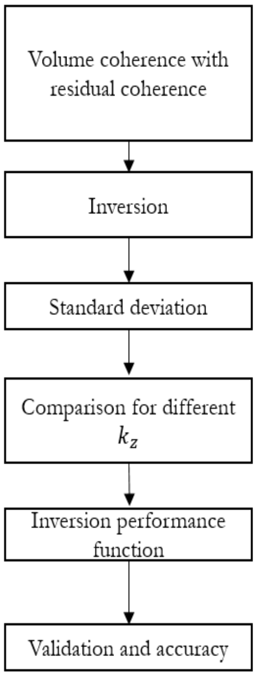

Figure 5. Methodology for optimization of inversion using a range of k_z

Tree heights are estimated by inversion with the k_z calculated from system metadata information. The statistics are studied from residuals, root mean square errors followed by calculation of standard deviation. From the acquired information, a range of k_z value is computed which is assumed to resolve the inaccuracies observed in the tree height estimation. Using this range of k_z values with the existing InSAR dataset pairs the tree heights are estimated. The estimated tree heights obtained from the SAR geometry are compared with tree heights obtained from simulated k_z to check if this provide optimal estimation of tree heights in the study area.

3.3. Validation and Accuracy Assessment

For the comparative study of estimated forest height and the field collected forest height statistical measures are used. The linear model fitting is done for the field measured heights and model derived heights. Coefficient of determination (R^2) and root mean square error (RMSE) are studied to analyse the reliability of the model. The root mean square error is calculated by:

$$\text{RMSE} = \frac{\sqrt{\sum_{i=1}^{n} (H_i^m - H_i^f)^2}}{\text{n}} \tag{17}$$

Where H^m is the height estimated from inversion and H^f is field observed height and n is the number of samples. Residuals are calculated from the difference between estimated values from inversion and field observed values at the same location. Small value of RMSE means that the model is highly reliable.

The accuracy percentage is assessed to find the average accuracy of the modelled output. It is calculated by:

$$A = \left[1 - \frac{1}{n}\sum_{i=1}^{n} \frac{\left|H_i^m - H_i^f\right|}{H_i^f}\right] \times 100 \tag{18}$$

The higher values of the accuracy percentage means how close are the modelled estimates to the field retrieved heights. These statistics are used to assess the dependability of inversion models. The estimation is performed using both coherence amplitude and three-stage inversion and the accuracy is assessed with respect to field data. The results are discussed in the following chapter.

4. STUDY AREA AND DATASET

The area for this research is Barkot and Thano forests located in the state of Uttarakhand, India at the foothills of Himalaya. Located between the Shivalik and Garhwal ranges of Himalayas, these areas are surrounded by the cities of Dehradun, Haridwar, and Rishikesh. The Ganga River flows along the eastern part of the study area. Sal (*Shorea robusta*) is the predominant species of tree in these forested areas. There are few other species of trees in the area like Teak (*Tectona grandis*), Sissoo (*Dalbergia sissoo*) and Khair (*Senegalia catechu*). Sal forest has dense canopy and broad leaves which exhibit high volume decorrelation. Easy accessibility and majorly mature foliage made the area most suitable for this study. The forests are surrounded by agricultural lands, urban areas and dry riverbed which show varied coherences.

Figure 6. Study Area

4.1. Test site

4.1.1. Thano forest

The forest of Thano (30.16° N-30.31° N and 78.13° E-78.30° E) lie under the jurisdiction of Forest Department, Uttarakhand. Covering an area of 117.75 km² it is a Sal forest with some traces of dry and moist mixed forests. The area is surrounded by agricultural land and human settlements. Road connectivity is good with main motor able metalled roads crossing from north to south and north to southwest namely, Rajpur-Thano Ranipokhari and Thano-Jolly Grant road. The Thano forest is highly impacted by the agrarian activities and pastoralism. The area has gentle to moderate slope with some seasonal streams flowing to the Song River. It is a forest abundant in moist Sal (*Shorea robusta*) and dry sal with some other species like 'karaunda' (*Carissa opaca*) and 'kathber' (*Zizyphus glaberrima*)(Singh, 2010). The climate in Thano varies from temperate to sub-tropical with mean annual temperature of 20°C.

Figure 7. Thano forest area

4.1.2. Barkot forest

The forest of Barkot (30.06°-30.17° N and 78.16° E-78.28° E) lie under the jurisdiction of Forest Department, Uttarakhand. Covering an area of 350 km² it is a mature Sal forest which shows less variation in tree heights. Road connectivity is good with main motor able metalled roads along the north to east namely, Dehradun – Rishikesh road. National highway 72 crosses some part of the study area. The forest has moderately dense canopy with the western part having density of around seventy percent. The area has a gentle slope ranging from 300m to 700m from south to north of the forest. Western parts of the forest are inaccessible due to highly active elephant corridors. It is a forest abundant in deciduous Sal (*Shorea robusta*) and Teak (*Tectona grandis*) with some other species like Amaltash (*Cassia fistula L.*) and Khair (*Acacia catechu (L.f.)*). The climate in Barkot varies from 23°C to 41°C in summers and 5°C to 23°C in winters. During the winter months of some years it faces snowfall.

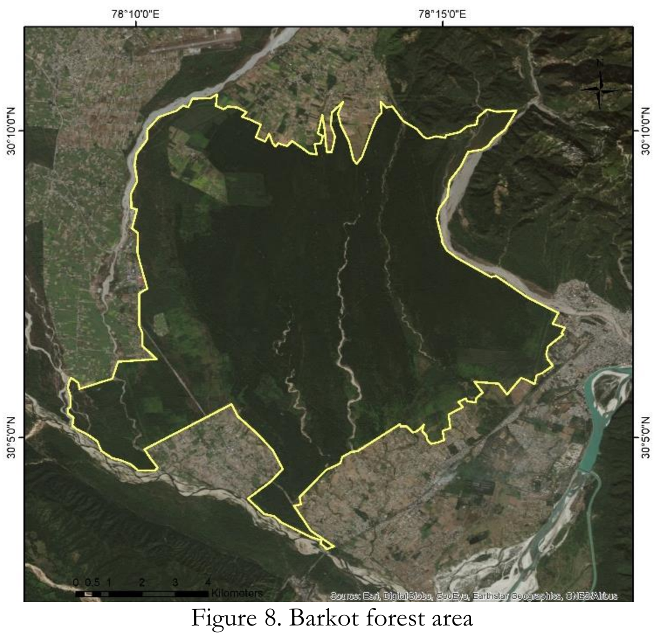

Figure 8. Barkot forest area

4.2. Dataset

For the study PolInSAR dataset are used and for validation purposes field data are used.

4.2.1. Satellite data

Quadratic polarised data of interferometric pairs from five dates between December 2014 and February 2015 are used in this study. The imagery were acquired by X band satellites TerraSAR-X and TanDEM-X in StripMap mode. The data is in single look complex (SLC) format with phase and amplitude information. The perpendicular baseline varies from 12.6 m to 734.85 m and temporal baseline varies from 0 to 66 days. Since X band has small wavelength it loses coherence with longer time thus subsiding the quality of interferometric pair. Therefore, from the datasets available, the pairs with minimum temporal baseline are used for this study. The near zero temporal baseline ensures that coherence is not reduced due to changes in time of scene acquisition. Small temporal baselines lead to low temporal decorrelation and prevent fluctuations in coherence and phase in interferometric pair. A detailed description of the dataset used is provided in Table 1.

Table 1. TerraSAR-X and TanDEM-X Dataset

Description	Dataset 1	Dataset 2	Dataset 3	Dataset 4	Dataset 5
Date of acquisition	19th December 2014	21st January 2015	1st February 2015	12th February 2015	23rd February 2015
Number of images	2	2	2	2	2
Perpendicular Baseline (m)	227.65	260.80	424.72	419.35	239.57
Height of Ambiguity (m)	16.53	14.43	8.87	8.98	15.71
Wavelength (cm)	3.10				
Polarizations	HH, HV, VH, VV				
Resolution (m)	3.06				
Pixel spacing (m)	1.36 × 2.86				

4.2.2. Field data

The field data used for validation of this study is adopted from previous studies which were collected during the month of March 2014 which was nearly during the same season as the satellite data acquisition. The majority of the field data have been collected for mature Sal trees which do not display drastic change in height over the years. The forest type maps acquired from the Forest Department were used to analyse the forest paths suitable for data collection. This data was utilized for strategizing field data collection. Field data was collected from 100 square plots with sides of 12.5 m spread over both the forested areas. The measurements of average tree height in each plot was calculated and used for accuracy assessment. The average tree height is between 15 m and 29 m. The devices used for this were a hand held Trimble Juno SB GPS receiver for geo-location information and a Criterion RD1000 Laser Dendrometer aided with Leica Disto D8 Laser Distance meter for tree height measurement (Kumar et al., 2017). Accessibility to different parts of the forest was a major criteria for the selection of plots for field data acquisition. The spatial coverage of Sal was found to be the highest in these area followed by dry and mixed forests, *khair-sisso* and other species. Since majority of the plots were covered with Sal forest the canopy density impacted the positional accuracy of GPS systems. Data collected from 100 plots in both Barkot and Thano forest as shown in Figure 9. From the available average tree heights the predominant average height of Sal tree is between 20 to 25 m. Table 2 shows species of the field data collection for all available plots.

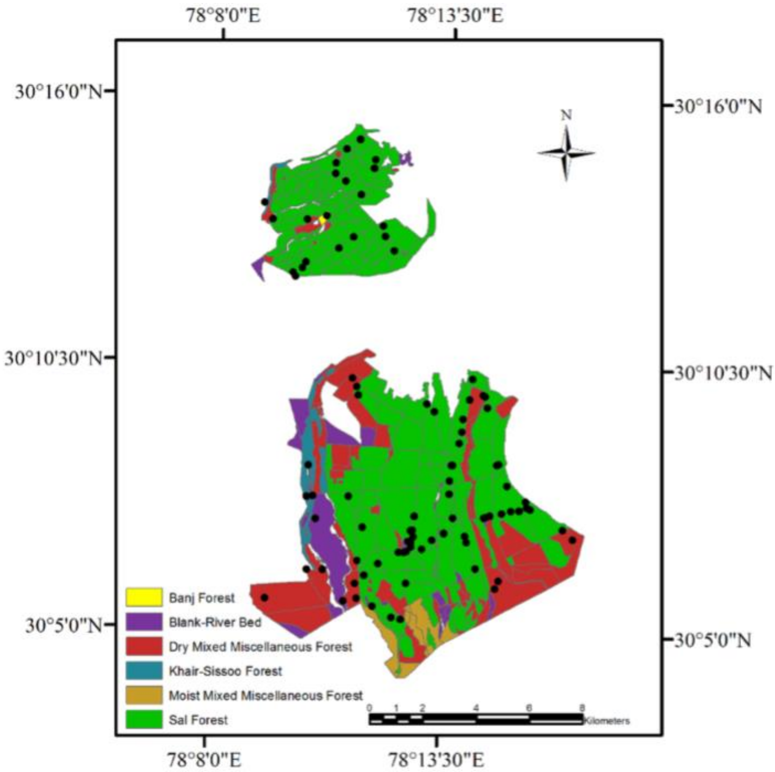

Figure 9. Forest class map with field plots for validation (Source: Kumar et al., 2017)

Table 2. Field plot tree species (Source: Kumar et al., 2017)

Forest species	Number of plots
Sal (*Shorea robusta*) forest	77
Dry mixed miscellaneous forest	16
Khair-sissoo (*Acacia catechu*, *Dalbergia roxburghii*) forest	5
Moist mixed miscellaneous forest	1
Banj (*Quercus leucotrichophora)* forest	1

4.3. Software

For processing and analysis of the data following software have been used:

- Sentinel-1 Toolbox (SNAP v 4.0) developed by European Space Agency (2016) is used for software data pre-processing and k_z calculation.
- Polarimetric SAR Data Processing and Education Toolbox (POLSAR pro v 5.1.1) from Institute of Electronics and Telecommunications of Rennes, University of Rennes, 2016 is used for flat earth removal, coherence estimation and interferogram generation.
- ArcGIS (ArcMap v 10.1) developed by ESRI is used for visualizing height maps.
- ENVI Classic 5.0 is used for the analysis of coherence and height values of forest form different models.
- R-Studio (R Core Team, 2015) is used for validation and accuracy assessment.

5. RESULTS AND ANALYSIS

The methodology mentioned in Chapter 3 is applied to estimate the forest heights using the coherence amplitude inversion and the three-stage inversion (Subsection 3.1.8). The modelled outputs are compared with the field data to study the accuracy of estimated tree heights. It is found that by altering the spatial baseline the estimation accuracy varied vastly. The overall accuracy for all the datasets improved when simulated k_z are implemented irrespective of the inversion algorithm used. The results obtained and their analysis is discussed in the following sections.

5.1. Coherence calculation

For calculation of the complex coherence, co-registration of all the available image pairs is performed to collocate areas in both images. For the purpose of co-registration 2000 ground control points are used (default in SNAP v4.0 toolbox). Coarse co-registration is performed with a window size of 128 × 128 followed by fine co-registration with a window size of 32 × 32 which is supposed to improve coherence between an image pair. The fine co-registration process takes into account the cross correlation between the master and slave images for the given window size. Then, the vertical wavenumber is calculated while considering the SAR system geometry. To eliminate the effect of temporal decorrelation data pairs with minimum temporal baselines are used. Since the study area has negligible undulations the terrain does not have significant effect on the value of k_z. A detailed description of topographic variation with k_z is presented in Appendix 2. The wavenumber are calculated for different values of effective baseline and are further used for height estimation.

The interferogram of the image pairs are generated after removal of the flat earth phase. Figure 10 shows the interferogram for the study area where undulations in the terrain and river channels have different fringe appearance than the surroundings. The forested areas show very small fringe pattern. The phase information from the interferogram is necessary for the further calculation of complex coherence and forest height estimation.

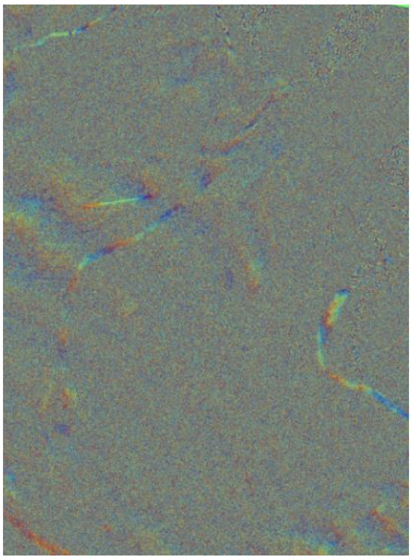

Figure 10. Interferogram of HV polarized images with larger fringes for gentle changes in the topography near river bed

As discussed in Subsection 3.1.4, the coherence matrix [T_6] are generated from the scattering matrices of the image pair. The [T_6] matrix contains entire polarimetric and interferometric information of the PolInSAR data. The information from different scattering mechanisms are observed from the Pauli basis image as shown in Figure 11. The river Ganga is observed as a dark body due to low reflection towards the receiver with Rishikesh city to the east showing double bounce scattering.

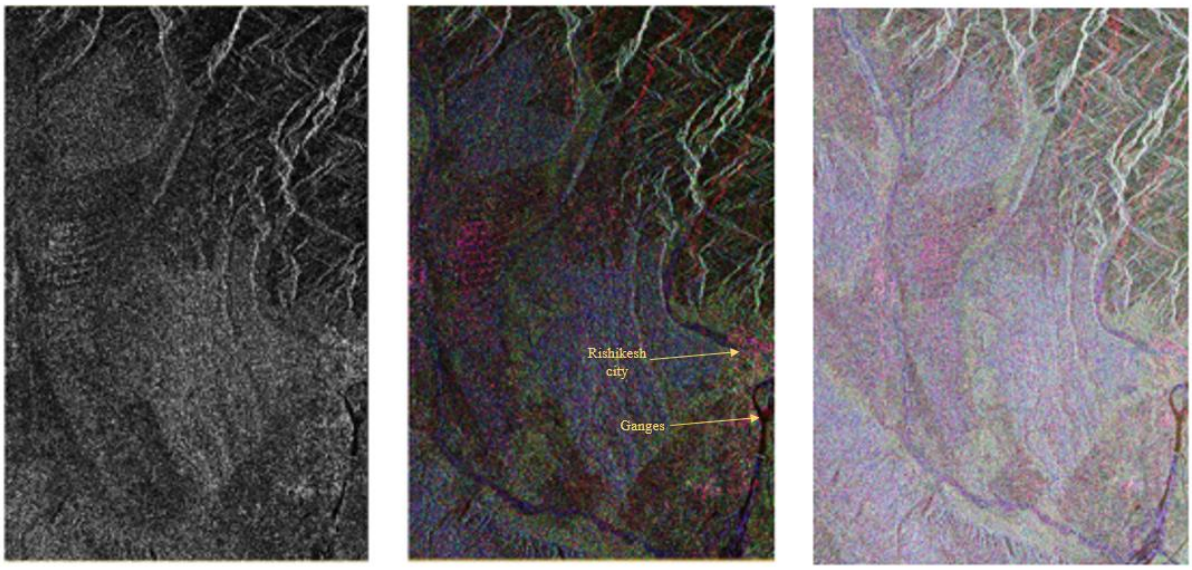

Figure 11. Single polarization HH image vs Colour composite Pauli basis backscatter image vs Pauli basis after [T6] generation with different scattering mechanisms (blue=surface scattering, red=double bounce scattering, green= volume scattering).

The water bodies display surface scattering with forested areas showing volume scattering from canopy, surface scattering from forest ground and double bounce from the tree trunks and ground interaction. The noise observed is due to volume decorrelation in the vegetated areas and forest. The complex coherence is observed to impart similar information about the features from the scattering mechanisms observed as obtained from the colour composite backscatter image.

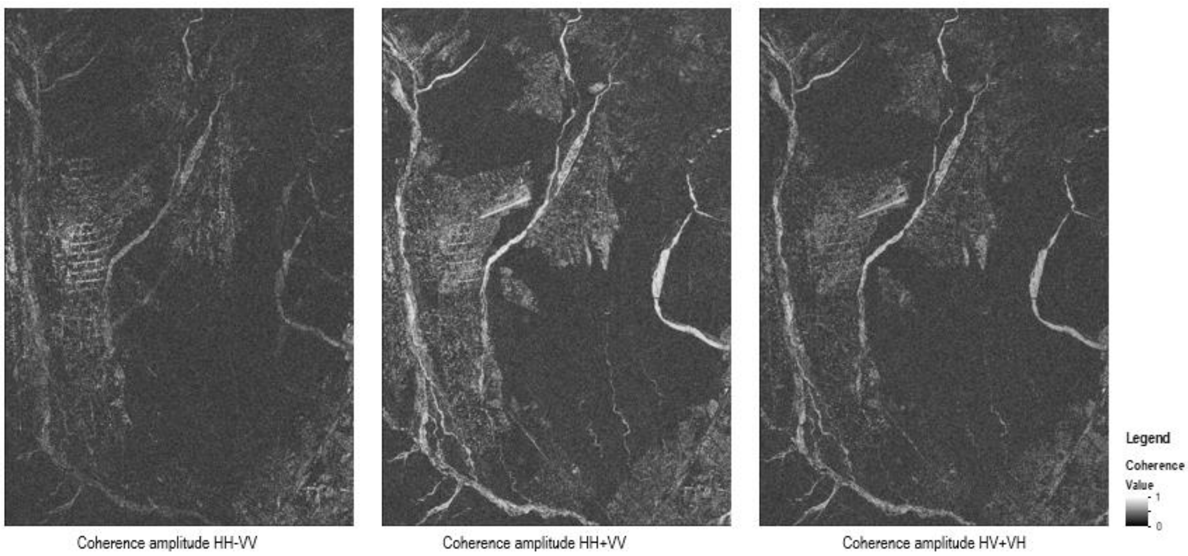

Figure 12. Coherence images of Pauli basis with high coherence observed in runway, urban areas and dry riverbed whereas low coherence observed in forested areas.

The complex coherence is calculated from the [T_6] matrix using equation (4). The coherence amplitude image generated is a greyscale image as shown in Figure 12. For calculation of coherence, window size should be mentioned for the averaging process around the pixel being considered. The boxcar filter of window size 11×11 is adopted for the estimation process. This increases the size of the resolution cell and minimizes difference between actual coherence and estimated coherence (Cloude, 2005). The coherence amplitude image shows very low coherence for the forest area and high coherence for features like dry riverbed and runway. The low coherence in forested regions is due to dissimilar volume decorrelation in different polarization.

The data acquired by TerraSAR-X and TanDEM-X are noisy and the variations in the coherence is not solely owing to polarization dependent scattering from forested areas but also due to speckle. This is observed from the coherences obtained in forested and non-forested areas. The coherence is found to be dissimilar for different polarization and different pairs of PolInSAR datasets. A range profile comparison for coherence acquired at different SAR geometry is shown in Figure 13.

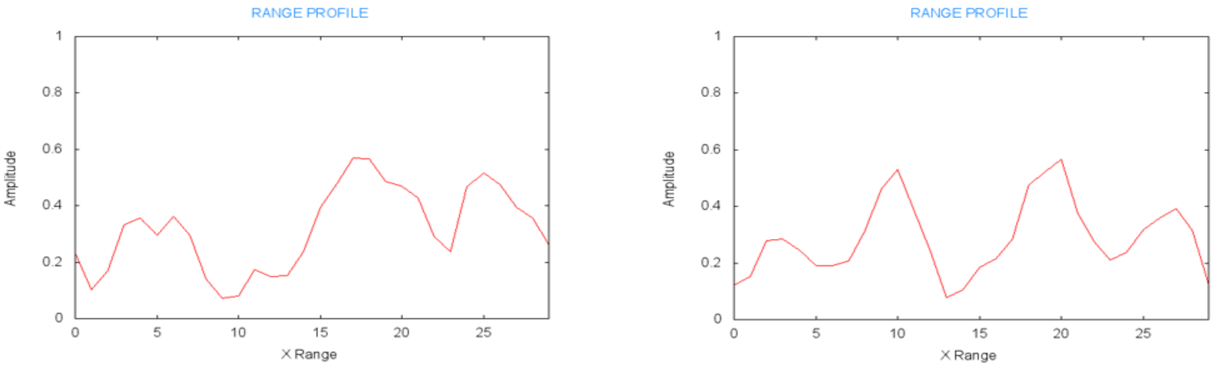

Figure 13. Coherence information for dataset with mean k_z value 0.25 (left) and 0.15 (right) for the same area within forest show that coherence changes with change in k_z

It shows that for the same area the value of coherence varies depending on the acquisition parameters thus, it reaffirms the findings of Kugler et al., (2015). Here overall low coherence is observed due to volume decorrelation with some variations observed for few of the forest pixels. This supports in deducing that the coherence which depends on the received SAR signals and eventually height estimation depends on the SAR geometry.

5.2. Estimation of tree height

The complex coherences are analysed to find the polarization channels with best representation of volume scattering and surface scattering. For coherence amplitude inversion, which calculates the difference in coherence from top and bottom of canopy structure, the HV+VH coherence for forest top phase and HH+VV for ground phase information is used. It can be observed from the colour composite coherence image of the Pauli basis polarization state, as in Figure 14.

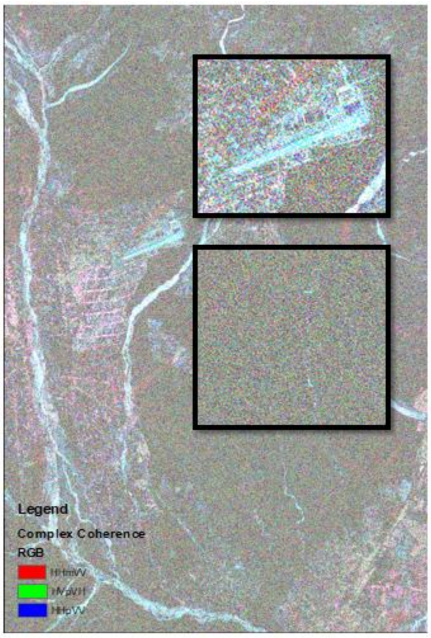

Figure 14. Colour composite of coherence in Pauli basis showing urban features (top) and vegetation (bottom) exhibiting different scattering mechanisms

The areas with high volume scattering like forests are shown in green with some noise which could be due to different physical properties. The regions where the SAR signals penetrate the forest display surface and double bounce scattering.

The coherence amplitude inversion exhibits underestimation of forest heights. Figure 15 shows the forest height map retrieved from two polarization coherences of Pauli basis. Estimated tree heights are in the range of 3.6 m to 15.4 m as shown in the figure. The average accuracy observed is low indicating the poor performance of the model for the particular dataset.

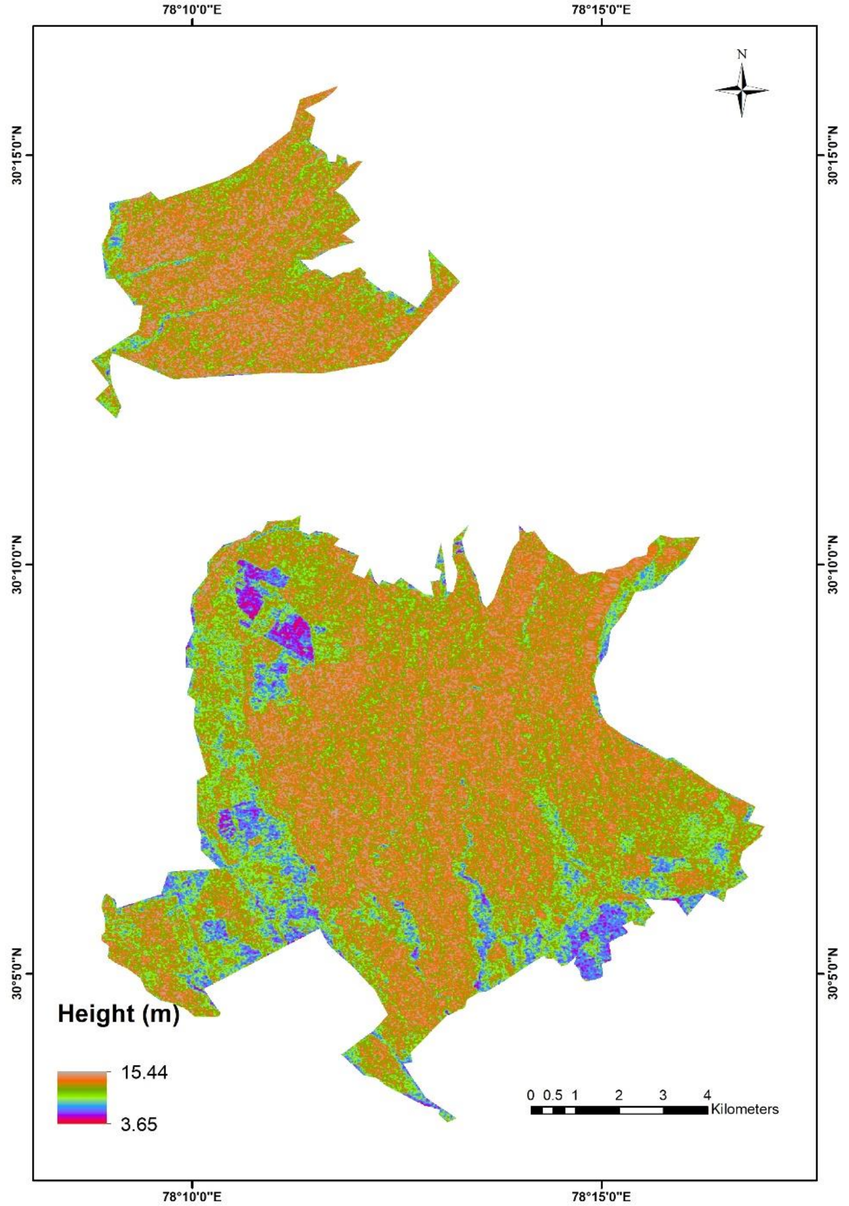

Figure 15. Coherence amplitude inversion height with HV+VH for volume scattering dominated coherence and HH+VV for surface scattering dominated coherence (23rd February 2015). The tree heights range between 3.65-15.44 m.

The maximum tree height retrieved over the forested area from both coherence amplitude inversion and three-stage inversion are comparable to the $\mathcal{H}\sigma\mathcal{A}$ calculated from SAR geometry. Similar observation is obtained from all the datasets. From Equation (3), the small value of $\mathcal{H}\sigma\mathcal{A}$ results in high value of k_z which is responsible for change in phase scale due to small heights causing underestimation of tree heights. Table 2 shows the statistics of estimated tree height for data pair (23rd February 2015) using coherence amplitude inversion. The tree height estimates are resampled to equal the plot size of field data. The forest height validation for 100 plots results in root mean square error of 1.44 m with an accuracy of only 50 %. The scatter plot of coherence amplitude inversion derived tree height with field data suggests weak correlation at 0.278.

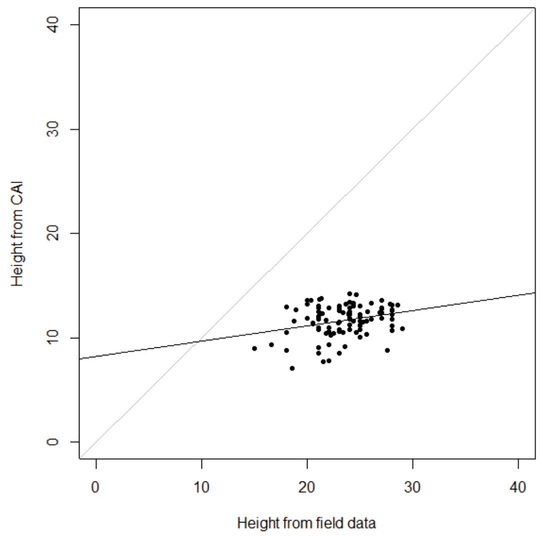

Figure 16. Coherence amplitude inversion (CAI) at perpendicular baseline=239.57 m, HoA = 15.71 m, Mean k_z= 0.40. The black solid line is the best-fit line and grey solid line is the 45° line.

Table 3. Coherence Amplitude Inversion (using SAR geometry) retrieved tree height statistics

Statistics (Coherence Amplitude Inversion)
Coefficient of determination (R^2) 0.0768
p- value 0.005
Correlation Coefficient (R) 0.278
Root mean square error (RMSE) (m) 1.44
Average Accuracy Percentage (%) 50.38

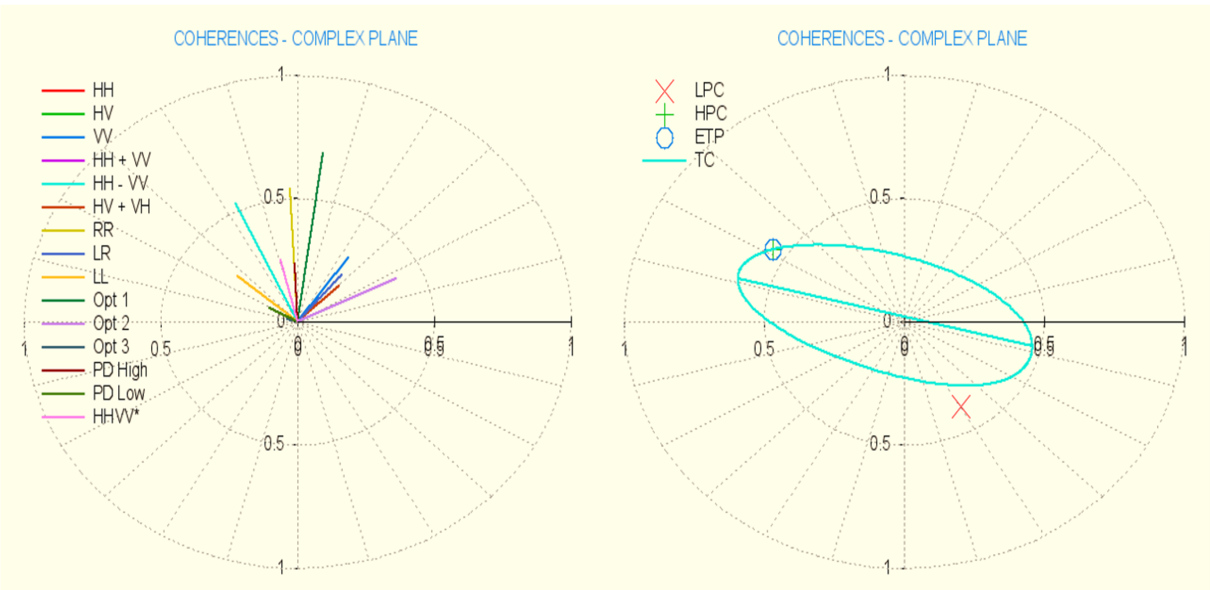

(a) (b)

Figure 17. Example of complex coherences plotted in complex plane for one pixel (a) to depict amplitude and phase information in different polarization basis as mentioned in the legend, and (b) to depict the coherence region with true coherence (TC), low phase centre(LPC), high phase centre (HPC).

In this study, three-stage inversion which uses the coherences in various polarization basis for tree height estimation has also been performed. The complex coherences are plotted in a unit circle as shown in Figure 17. The true ground phase and true volume coherence are identified from the unit circle as discussed in Subsection 3.1.8.2 using equations (14)-(16). The three-stage inversion exhibits overall underestimation of forest heights. Figure 18 shows the forest height map retrieved from three-stage inversion. Estimated tree heights are in the range of 0 m to 14.43 m as shown in the figure. The average accuracy observed is low indicating the poor performance of the model for the particular dataset.

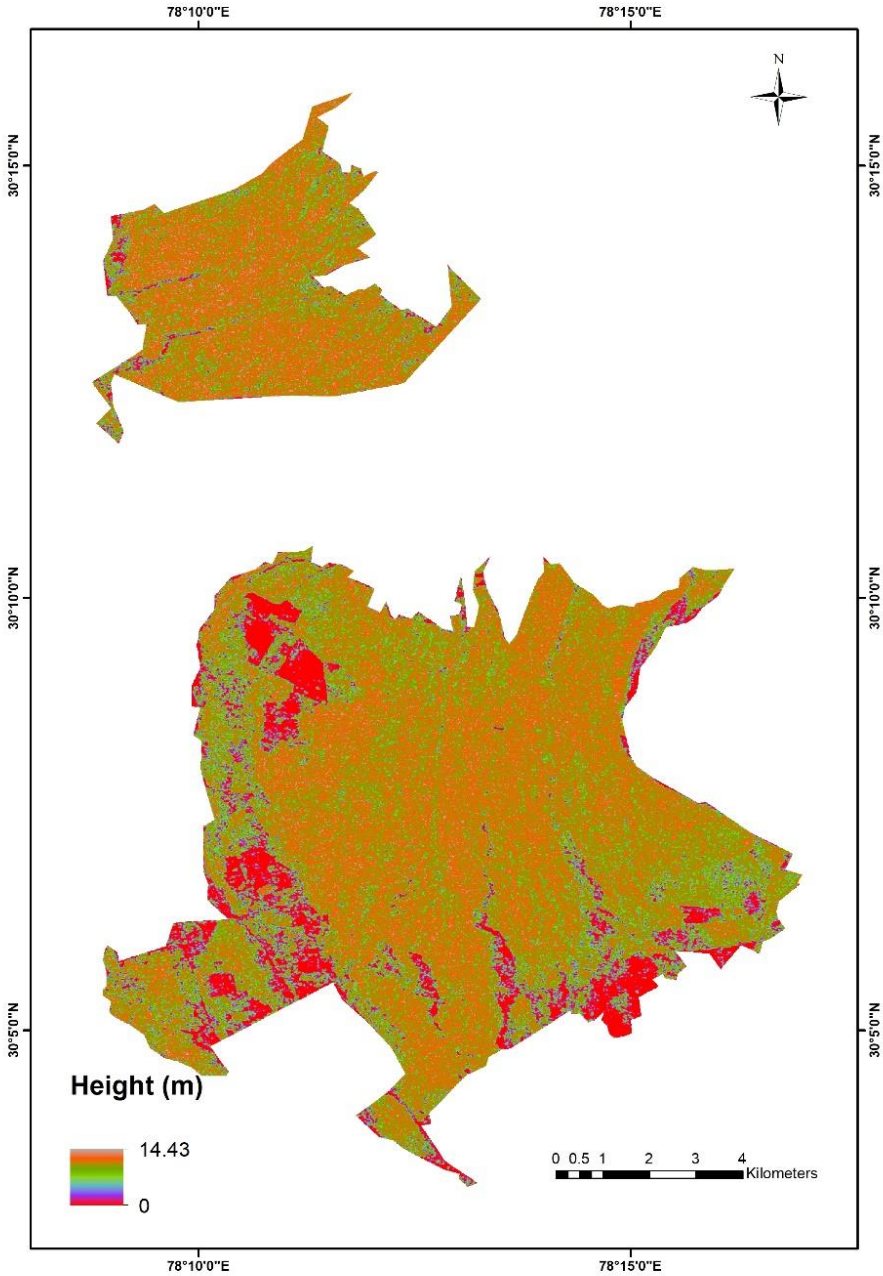

Figure 18. Three-stage inversion forest heights for single dataset (23rd February 2015). The tree heights range between 0-14.43 m.

Table 3 shows the statistics of estimated tree height for data pair (23rd February 2015) using three-stage inversion. The forest height validation for 100 plots results in root mean square error of 2.47 m with an accuracy of only 42.8 %. The scatter plot of coherence amplitude inversion derived tree height with field data suggests weak correlation at 0.31. It is observed that three-stage inversion tree height estimates have relatively higher correlation with field retrieved data than coherence amplitude inversion despite highly underestimated tree heights at certain plots. High underestimations are mainly observed at plots with agricultural land with low average tree height. The maximum observed height is determined by the observed $\mathcal{H}o\mathcal{A}$ as shown in Equation (3). Tree heights estimated from coherence amplitude inversion in the study area are taller than the three-stage inversion. Comparative analysis of tree heights from 150 random samples are shown in Figure 20. The tree heights retrieved by all datasets are underestimated due to the low $\mathcal{H}o\mathcal{A}$ observed from the SAR geometry.

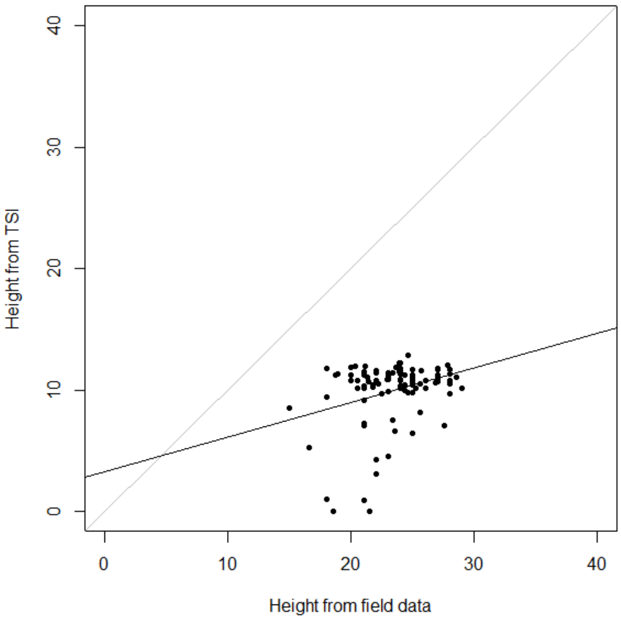

Figure 19. Three-stage inversion (TSI) at perpendicular baseline=239.57 m, HoA = 15.71 m, Mean kz=0.40 The black solid line is the best-fit line and grey solid line is the 45° line.

Table 4. Three-stage Inversion (using SAR geometry) retrieved tree height statistics

Statistics (Three-stage Inversion)
Coefficient of determination (R^2) 0.0962
p- value 0.001
Correlation Coefficient (R) 0.31
Root mean square error (RMSE) (m) 2.47
Average Accuracy Percentage (%) 42.88

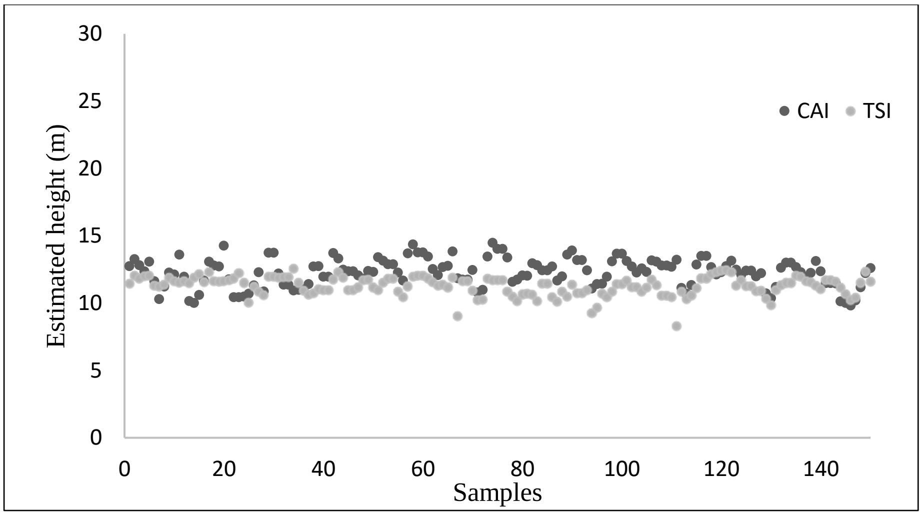

Figure 20. Comparison of tree height estimates from Three-stage inversion (TSI) and Coherence amplitude inversion (CAI) for transect across the study area.

Table 5 shows the statistics of the estimated height from the available datasets. The estimated tree heights are saturated around the height of ambiguity. This necessitates the use of minimum height of ambiguity comparable to the tallest tree heights obtained from the field data. For this, a priori information of the stand height is crucial for the estimation of tree heights in any study area.

Table 5. Maximum tree height (m) from inversion for entire study area

Model	**19th December 2014**	**21st January 2015**	**1st February 2015**	**12th February 2015**	**23rd February 2015**
Coherence amplitude inversion	16.25	14.18	8.73	8.86	15.44
Three-stage inversion	15.21	13.60	7.99	8.86	14.43
HoA (from data)	16.53	14.43	8.87	8.98	15.71

5.3. Impact of vertical wavenumber on inversion

The forest heights are estimated from the complex coherence while considering zero temporal decorrelation and total volume decorrelation. For each data pair coherence is calculated and tree height inversion is performed to find the estimated tree heights. While using a range of vertical wavenumber k_z from 0.35-0.75 radm^{-1} for tree heights ranging between 15-29 meters measured from field data, it is observed that the standard deviation of the estimated tree height decreased with increasing k_z values. Mean k_z of 0.37 radm^{-1} returns a standard deviation of 1.46 m whereas mean k_z of 0.70 radm^{-1} results into a standard deviation of 0.6 m. As discussed in Subsection 2.2.2, the coherence level is reduced at high values of k_z and results in underestimated tree heights. The coherence increases at low values of k_z which can be achieved by implementing a smaller effective baseline, from Equation (1). Simulation of smaller effective baseline are expected to improve coherence and estimation of tree heights.

Section 5.2 suggests that the maximum estimated tree height is similar to the $\mathcal{H}\sigma\mathcal{A}$ considered from the SAR geometry. For $\mathcal{H}\sigma\mathcal{A} = 15.71$ m (mean k_z= 0.4 radm^{-1}) the estimated tree heights show correlation of 0.60 (at p-value < 0.05) with field retrieved heights ranging between 15 to 20 meters and very low correlation of 0.18 with field heights ranging between 20 to 29 meters. Similar pattern is observed for $\mathcal{H}\sigma\mathcal{A} = 16.53$ m (mean k_z= 0.35 radm^{-1}). It is also established that k_z scales both interferometric phase and coherence of volume scatterers. Previous studies have shown that for a gradual increase in value of k_z the sensitivity of coherence to height is reduced and for a gradual decrease in value of k_z there are overestimated heights (Kugler et al., 2015). For the ideal situation, estimates equal the true tree heights, to achieve this the value of $k_z$is replicated to match the ideal k_z range.

5.4. Estimation of tree height with simulated wavenumber

Across the study area, linear models are derived to describe the relationship between tree heights estimated with simulated k_z (at $\mathcal{H}\sigma\mathcal{A}$ = 60 m) and field retrieved tree heights. The estimated mean tree height in the plot with minimum mean field height of 15 m is 35.80 m for coherence amplitude inversion and 35.34 m for three-stage inversion. Whereas, for the plot with maximum mean field height of 29 m the estimated heights are 43.44 m for coherence amplitude inversion and 38.28 m for three-stage inversion. Clearly, the tree heights are overestimated for both coherence amplitude inversion and three-stage inversion for $k_z = 0.1$radm^{-1}. Table 6 shows the validation statistics for 100 field plots. For every dataset, the tree heights are overestimated with both the inversion techniques. This strengthens that k_z should be such that it is able to scale the maximum available tree height for an accurate estimation while using the appropriate$\mathcal{H}\sigma\mathcal{A}$.

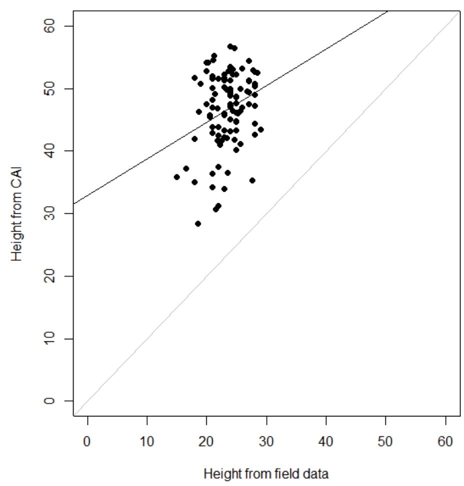

Figure 21. Coherence amplitude inversion at kz=0.10. The black solid line is the best-fit line and grey solid line is the 45° line

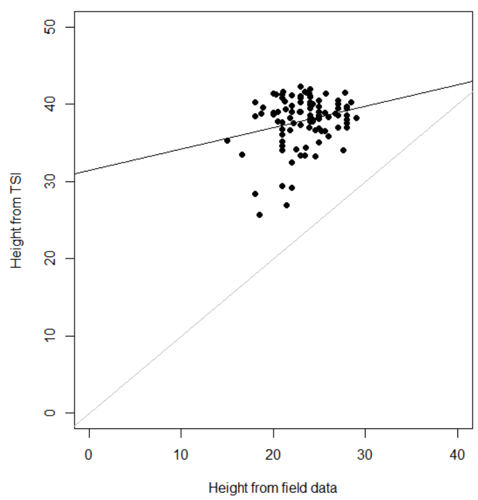

Figure 22. Three-stage inversion at kz=0.10. The black solid line is the best-fit line and grey solid line is the 45° line

Table 6. Tree height estimation statistics for simulated kz=0.10

Statistics (Coherence amplitude inversion)
Coefficient of determination (R^2) 0.0768
p- value 0.005
Correlation Coefficient (R) 0.31
Root mean square error (RMSE) (m) 5.75
Statistics (Three-stage inversion)
Coefficient of determination (R^2) 0.0595
p- value 0.01
Correlation Coefficient (R) 0.24
Root mean square error (RMSE) (m) 3.13

The correlation between tree heights estimated with simulated k_z (at $\mathcal{H}o\mathcal{A}$ = 30 m) and field retrieved heights are shown in Figure 23 and Figure 24. Across all the datasets, the model slopes are similar ranging from 0.15-0.28 for coherence amplitude inversion and 0.11-0.20 for three-stage inversion. The coherence amplitude inversion shows a relationship of $R^2 > 0.04$ and p-value <0.05 (n=100) for four datasets used. 19th December, 2014 dataset shows a relationship of $R^2 = 0.02$ and p-value > 0.05 (n=100).

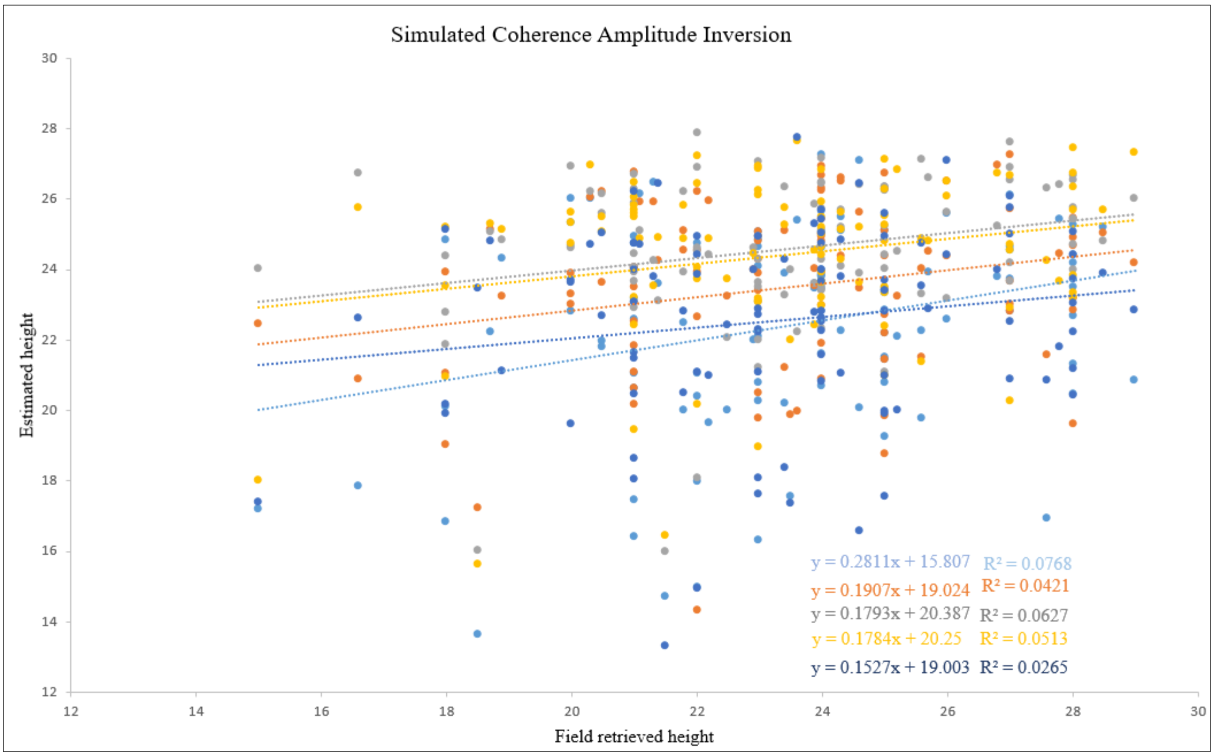

Figure 23. Coherence amplitude inversion heights (m) with simulated wavenumber correlation plot with field data

The detailed statistics of the mean tree height estimates from coherence amplitude inversion with simulated wavenumber for 100 plots are shown in Table 6.

Table 7. Coherence amplitude inversion: Detailed statistics of tree height (m) estimates for 100 plots

Statistics	Field data	19th December 2014	21st January 2015	1st February 2015	12th February 2015	23rd February 2015
Maximum	29	27.79	27.27	27.87	27.65	27.25
Minimum	15	13.29	10.81	16.01	15.64	13.64
Mean	23.44	22.58	23.49	24.58	24.43	22.39
Standard deviation	2.84	2.67	2.64	2.03	2.24	2.87

The three-stage inversion shows a relationship of $R^2 > 0.04$ and p-value <0.05 (n=100) for four datasets. 12th February, 2015 dataset shows a relationship of $R^2 = 0.025$ and p-value > 0.05 (n=100). There are no significant differences (p-value >0.05) in majority of the dataset suggesting no change in tree heights over the time span.

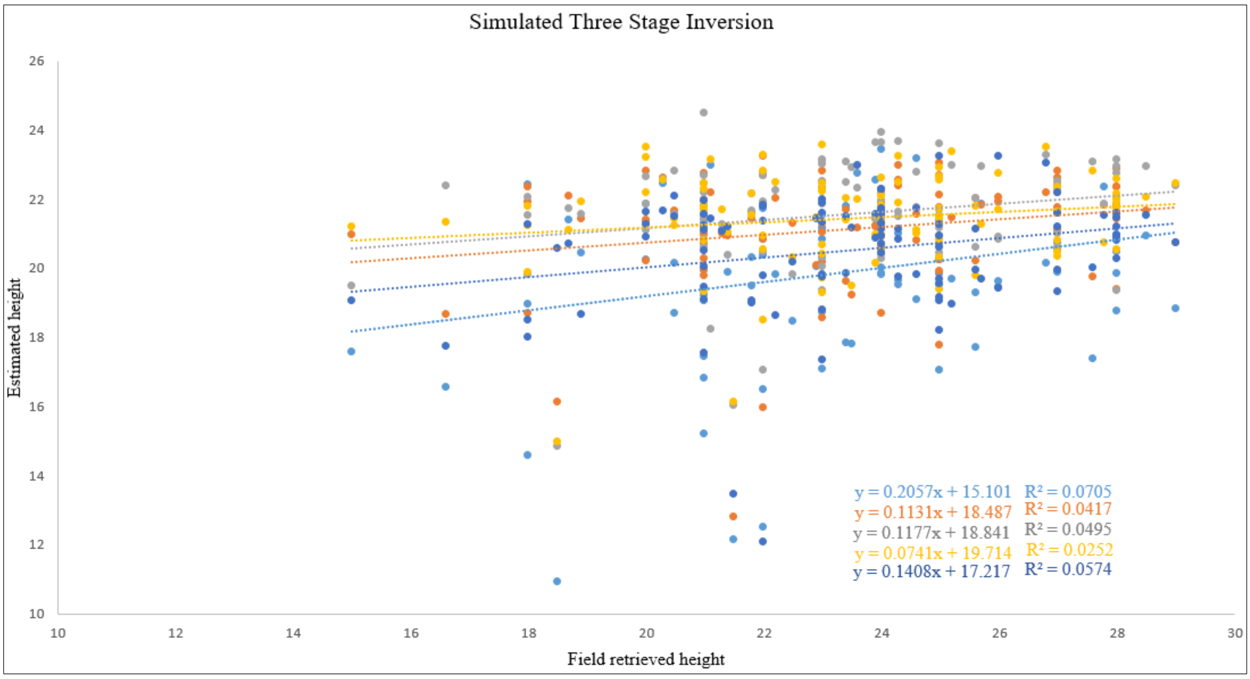

Figure 24. Three-stage inversion heights (m) with simulated wavenumber correlation plot with field data

The detailed statistics of the mean tree height estimates from three-stage inversion with simulated wavenumber for 100 plots are shown in Table 7.

Table 8. Three-stage inversion: Detailed statistics of tree height (m) estimates for 100 plots

Statistics	**Field data**	**19th December 2014**	**21st January 2015**	**1st February 2015**	**12th February 2015**	**23rd February 2015**
Maximum	29	23.25	23.25	24.49	23.56	23.44
Minimum	15	12.08	12.79	14.84	14.90	10.92
Mean	23.44	20.51	21.13	21.59	21.45	19.92
Standard deviation	2.84	1.67	1.57	1.50	1.32	2.20

The tree height maps of estimated heights from coherence amplitude inversion and three-stage inversion using simulated k_z is presented in Appendix 3.

5.5. Validation and accuracy assessment

The tree heights estimated using simulated k_z = 0.21 radm^{-1} are relatively accurate compared to the tree heights estimated using SAR geometry. The coherence amplitude inversion tree heights show root mean square error less than 3 m and average accuracy of more than 85 %. The three-stage inversion tree heights show a lower root mean square error less than 2.5 m and average accuracy of more than 83 % for all the datasets. There is underestimation in the tree heights on some of the plots out of the total 100 plots used for the validation.

For all the datasets the average accuracy of the estimated tree heights increases by almost 40 % when mean k_z = 0.21 radm^{-1}. The relationship between estimated tree height and field data improves for three-stage inversion from when k_z calculated with SAR geometry is used. Figure 25 and Figure 26 shows the comparison of linear models relating estimated tree heights.

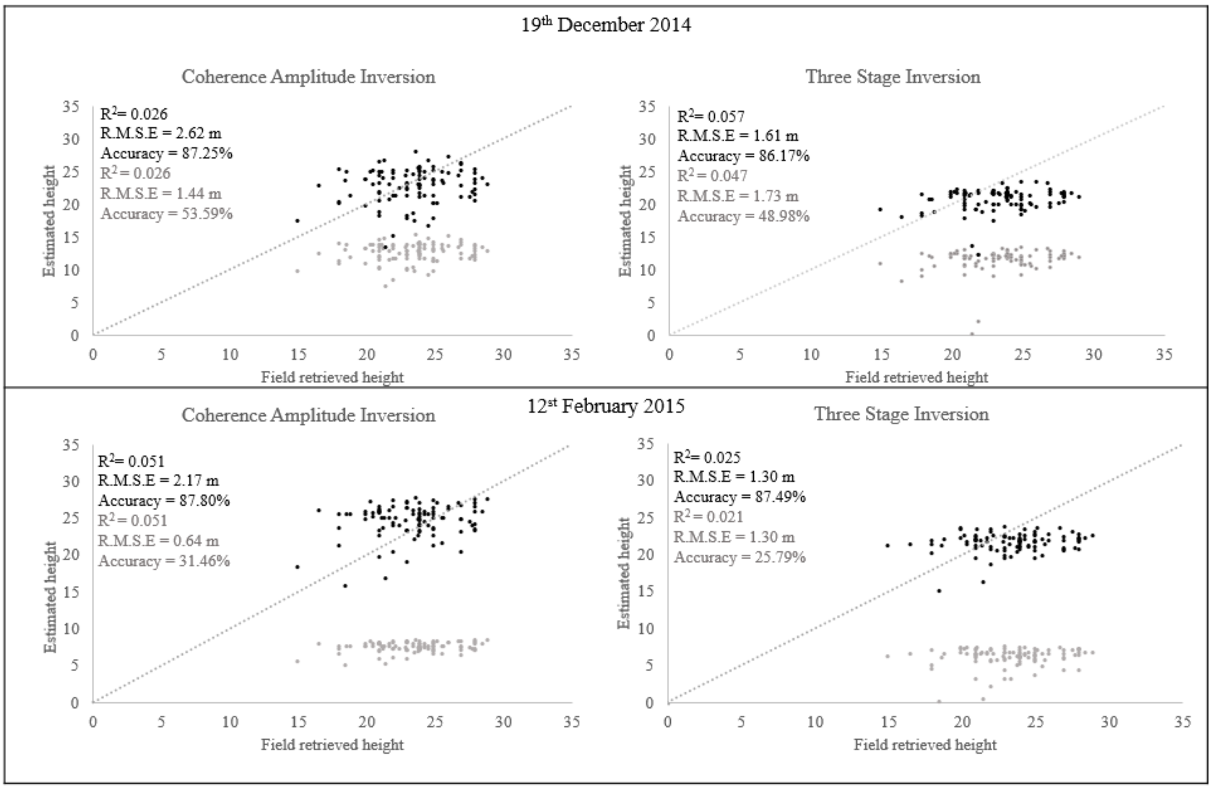

Figure 25. Scatterplot of tree height estimated from SAR geometry (in grey) and simulated wavenumber (in black) vs field data for two datasets: 19th December 2014, 12th February 2015 (p-value ≈0.1) (unit = meters)

The root mean square error for coherence amplitude inversion using simulated k_z ranges from 1.96 m to 2.76 m and for three-stage inversion ranges from 1.3 m to 2.11 m which is majorly higher than the error obtained by SAR geometry for all datasets. The average accuracy for tree heights estimated with simulated k_z ranges from 83 % to 88 %. There are few plots where underestimation remains even after simulation of wavenumber. These outliers are due to mixed vegetation in certain plots of data collection which affects the average tree height in the plot.

The correlation between estimated tree height and forest retrieved tree height for coherence amplitude inversion using k_z computed from metadata information ranges between 0.10 to 0.27 whereas correlation between estimated tree height and forest retrieved tree height for three-stage inversion using k_z computed from metadata information ranges between 0.14 to 0.30.

The correlation between estimated tree height and forest retrieved tree height for coherence amplitude inversion using simuated k_z ranges between 0.16 to 0.27 whereas correlation between estimated tree height and forest retrieved tree height for three-stage inversion using simuated k_z ranges between 0.15 to 0.26.

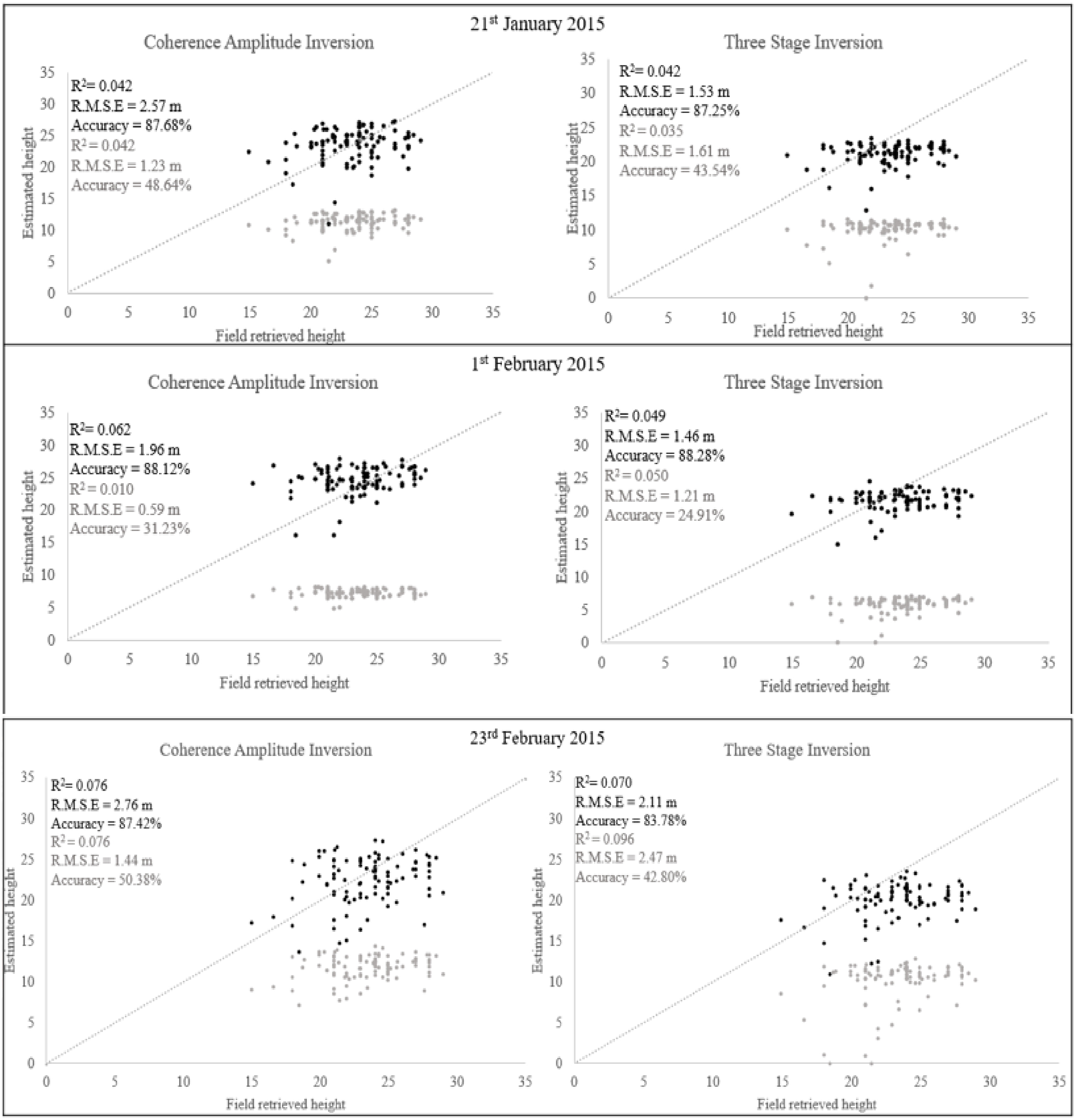

Figure 26. Scatterplot of tree height estimated from SAR geometry (in grey) and simulated wavenumber (in black) vs field data for three datasets: 21st January2015, 1st February 2015, 23rd February 2015 (p-value <0.05) (unit = meters)

From the Figure 25 and 26, the validation plots for tree height estimates with simulated wavenumber are noisier than the one with estimates from SAR geometry, but the overall accuracy of more than 80% and RMSE of less than 3 m are convincing. At some plots with zero estimated height improvement in height estimates is observed with simulated value over estimated tree heights from three-stage inversion using k_z.

The comparison between the results of tree height estimation suggest better overall accuracy of coherence amplitude inversion but higher RMSE than three-stage inversion. Residuals are calculated by subtracting estimated tree heights from the field data. Figure 27 shows the residuals of the estimated tree heights. The residuals obtained from three-stage inversion are less than the residuals obtained from coherence amplitude inversion suggesting a better performance of three-stage inversion.

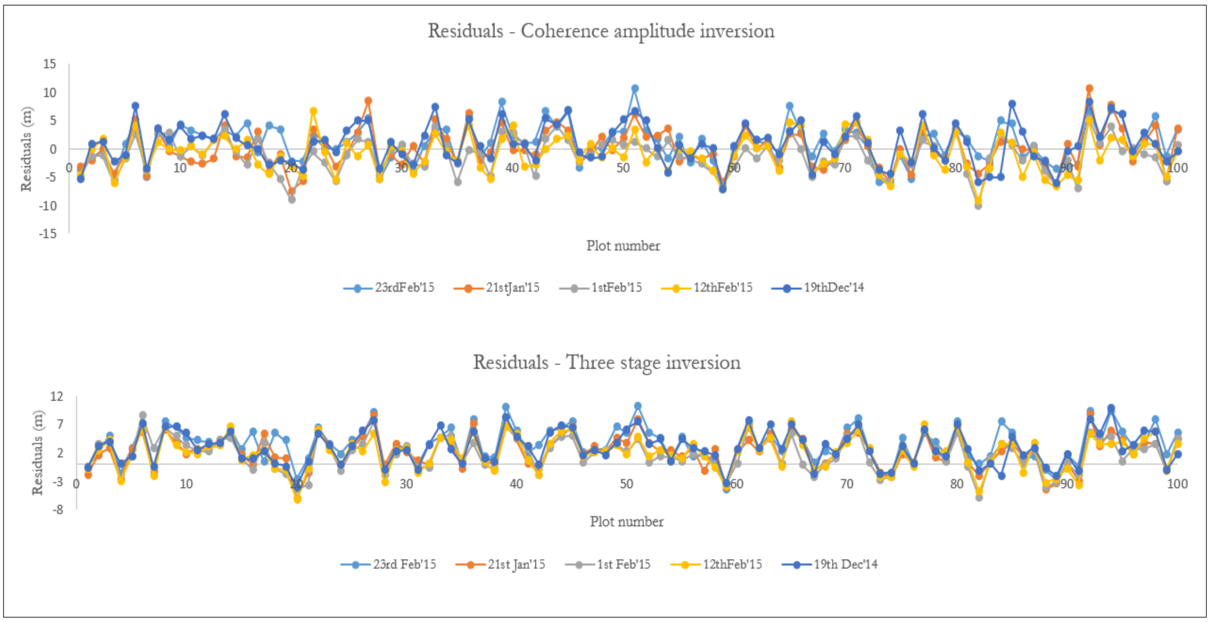

Figure 27. Scatterplot of residuals in tree height estimates from inversion using simulated wavenumber

The overall maximum residuals for coherence amplitude inversion is 10.68 and for three-stage inversion is 10.2.

The tree heights estimated from the inversion using different k_z values, calculated from product metadata and from the simulated k_z are compared to highlight a consistency amongst the estimated heights from both methods. The inversion heights are highly correlated with RMSE of approximately 1 m as shown in Figure 28.

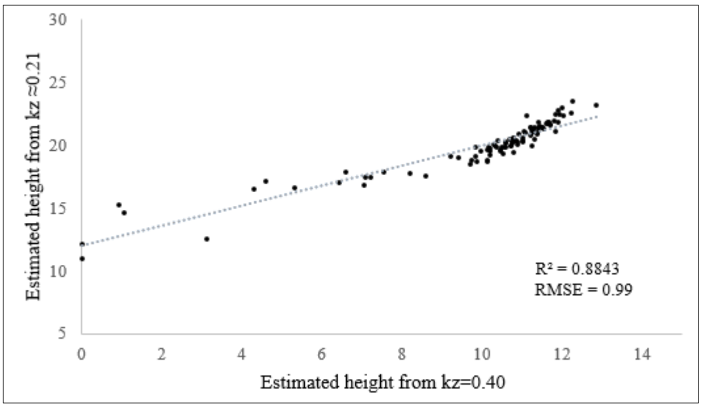

Figure 28. Comparison of forest height with kz=0.40 vs. kz=0.21 for 100 validation plots for 23rd February 2015 dataset.

Similarly, for all other datasets there exists a strong correlation between the estimated heights from both inversions.

6. DISCUSSION

The main objective of this research is to estimate forest height from PolInSAR inversion techniques and its optimization using simulated wavenumber. A discussion drawn from the obtained results in the previous chapter, a comparison with existing work and the constraints of this research are discussed in this chapter.

6.1. Coherence and volume scattering

The coherence observed in forested areas is low compared to the coherence in non-forested regions. Frequent change in their orientation, winds etc. make forests very unstable scatterers. The penetration of the incident SAR wave depends on the density of the canopy. The polarimetric and interferometric signature of the volume scatterer can be identified from the coherence region. The volume decorrelation in different polarization channels impact the shape of the coherence region. The forests present in the study area display low coherence overall for all polarizations. The cross polarized channels show comparatively higher coherence for forested areas than co polarized channels which strengthen the fact that scattering is dependent on the polarization of incident SAR wave. The coherence observed from two different InSAR pairs with different wavenumbers show variation suggesting that coherence is dependent on the baseline which confirms the findings of previous studies.

6.2. Forest height from SAR geometry

The forest height estimated from the SAR geometry displayed underestimation for all datasets. Maximum correlation between estimated and field measured tree height is 0.27 for coherence amplitude inversion and 0.30 for three stage inversion at p-value <0.05, which shows that the modelled height provide a feeble yet statistically significant relationship with the field measured height. The correlation can be associated to the resolution of the used dataset (Chen et al., 2016) and improves with upscaling resolution. The maximum estimated heights are similar to the $\mathcal{H}\sigma\mathcal{A}$ obtained from the metadata of the dataset. The maximum observed tree height estimation accuracy with coherence amplitude inversion is 53.59% and with three-stage inversion is 48.98% which is lower than that is observed with dataset with ideal baseline. This make the datasets unsuitable for tree height estimation and indicate the necessity of optimization. There is an observed inverse proportionality between perpendicular baseline and tree height estimation accuracy which further becomes a precursor in simulation of the ideal wavenumber.

6.3. Vertical wavenumber as a scale for height estimation

Previous studies have explored different inversion techniques to estimate tree heights. While the inversion performance strongly depend on decorrelation, topographic variation and the vertical wavenumber, the results suggest the importance of an appropriate value of k_z for inversion. Certain values of $k_z$are able to perform tree height estimation with improved accuracy for only a limited range of tree heights. Large k_z values underestimate tree heights, but for these k_z values estimated tree heights of smaller stands are nearer to field retrieved heights. This is in line with the findings of Lee et al., (2009). While the maximum observed tree heights are comparable to $\mathcal{H}\sigma\mathcal{A}$for all the datasets this helps identify the limits for the range of idealk_z. The k_z value adopted should be such that it supports in estimation of tree height while considering the topography of the region. Simulations with multiple baselines evidently help in achieving a range of $k_z$values for optimal inversion performance.

6.4. Forest height from simulated wavenumber

When forest height is estimated from a preferred range of k_z values, with $\mathcal{H}\sigma\mathcal{A} \approx 30$m, the correlation between estimated tree height and field measured forest height increases. Maximum correlation between estimated and field measured tree height is 0.27 for coherence amplitude inversion and 0.26 for three stage inversion. The validation of estimated tree height shows maximum RMSE of 2.76 m for coherence amplitude inversion and 2.11 m for three-stage inversion. The minimum accuracy is 87.25% for coherence amplitude inversion and 83.78% for three-stage inversion. The RMSE values obtained from the simulated k_z and by previous studies like Kugler et al., (2014) with X band dataset are alike. The observed RMSE is relatable to RMSE from dataset of the same area as found by Kumar et al., (2017) which was acquired with different microwave frequency. The residuals of estimated tree height show that the coherence amplitude inversion resulted in high dissimilar errors in estimation for all the datasets. The three-stage inversion errors are less noisy with a similar pattern for all the datasets thus implying the robustness of this inversion technique. This is in line with the findings of Cloude & Papathanassiou (2003). There are field heights which display large underestimation with SAR geometry but have reduced comparatively with the new method. There still remains underestimation but the overall tree height estimation is improved. The underestimations can be related to the mixed vegetation type in some of the plots used for validation.

The validation plots of the tree height estimates with field data suggest the prevalence of systematic uncertainties which can be removed by calibration of the linear models. The calibration can attempt to differentiate the systematic errors from non-systematic errors thus improving the precision of a model. Since the availability of field data is limited in this study the calibration could not be attempted as a significant measure. Pixel wise forest cover information if made available from LiDAR acquisitions can be useful as reference field data for the calibration of the linear model.

6.5. Limitations

There are some factors affecting the performance of the models and simulation approach in this research. While the simulation of kz such that $\mathcal{H}\sigma\mathcal{A} \approx \max(h_v)$ resulted in improved accuracy of tree height estimation there are fluctuations in observed tree heights due to the noise inherent in TerraSAR-X datasets. The noise could be speckle or thermal and affects the acquired image with granular dark and bright spots. Factors like the transmitted power, received signal determine the noise in a SAR system. Vegetation as a distributed target usually displays low backscatter and high signal to noise ratio thus impacting the radiometric resolution.

The penetration capability of X-band through the forest canopy determines its ability to estimate height. As the canopy density dictates the penetration the height estimates in mixed forest areas are inconsistent. While X-band had earlier proved to give good estimation of tree heights in sparse forest density, its inability to go through the wide canopied Sal (*Shorea robusta*) forest result in underestimated heights. The polarimetric property of the scatterers also influences the observed interferometric coherence and thus influencing the content of information available from PolInSAR inversion.

The classical inversion models implemented in this study have certain drawbacks. Both coherence amplitude inversion and three-stage inversion underestimates tree heights. Coherence amplitude inversion completely neglects the phase information and considers only the coherence amplitude. This technique makes the height estimate highly dependent on the forest density and structure. For this reason coherence amplitude inversion is not a robust technique. Three-stage inversion, although suggested by researchers to be a better technique strongly depends on the assumption that one polarization channel displays very low ground to volume scattering ratio to correctly estimate tree height which might not be the case in real scenario.

The accuracy of GPS positioning is impacted by the dense canopy which may alter the field validation results. This could be curbed to large extent by using LiDAR based validation. With LiDAR, data can be acquired from vast, inaccessible areas and form a large collection of field data set. Large number of in-situ data could strengthen the validation and calibration procedure which eventually can improve the overall analysis.

The SAR signals from distributed scatterers from within a resolution cell superimpose each other which make the decomposition of the scattering vectors necessary. PolInSAR is based on second order statistic coherency and covariance matrices with an assumption that scattering vectors following a complex Gaussian distribution. The assumption holds true for data with low or medium resolution but not always for high resolution data from TerraSAR-X and TanDEM-X. For non-homogenous natural areas the second order Gaussian statistics does not provide a good fit as studied by researches previously. This indicates higher order statistics could be implemented in future studies for better inversion results.

6.6. Final remarks

Even though X-band might not be the optimal choice for tree height estimation in Barkot and Thano forests the methodology implemented for PolInSAR inversion and optimization of tree height estimates by simulation of ideal wavenumber shows improved inversion results. The non-ideal baseline can successfully provide estimation outcomes with small errors for both coherence amplitude inversion and three-stage inversion attempted. The underestimation of tree heights suggest the future scope of improvement in the inversion techniques.

7. CONCLUSION AND RECOMMENDATION

The conclusion drawn from this research and future prospect of this in forest height monitoring is discussed in this chapter.

7.1. Conclusion

Forest monitoring is vastly demanded by institutions like forest authorities, governments, or non-government organizations to protect forests from illegal logging activities to ensure better forest management and to monitor carbon sinks. The quantitative information of forests like tree height is considered an important parameter for forest management. Forest parameter information collected manually from ground measurements are extremely challenging and time consuming. Remote sensing techniques for quantitative measurement of forest parameters are not very well explored. PolInSAR systems have been studied previously to estimate the quantitative parameters like forest height.

In this research, PolInSAR forest height estimation is established from X- band dataset acquired from TerraSAR-X and TanDEM-X. The study area has mature Sal trees with minimal height variation over time. For the estimation of height two widely used inversion techniques namely; coherence amplitude inversion and three-stage inversion are implemented. Factors which impact the estimation are baseline and decorrelations in the PolInSAR data. These factors build the basis for this research to improve tree height estimation method. While many studies have previously focussed on the different inversion techniques to optimize the tree height estimation, there are limited literature that suggests the role of vertical wavenumber to scale the optimization. Some studies had developed PolInSAR inversion based optimization methods with simulated datasets and implementation on real datasets (like L-band, P-band). This research work reflects some concepts from the previous works and originates a basic strategy to optimize PolInSAR inversion based tree height estimation with X-band datasets and non-ideal baselines.

All the TerraSAR-X and TanDEM-X orbits are not appropriate for generating height estimation through PolInSAR inversion techniques. Prior knowledge of the mean tree height in an area and the topography is essential for the optimal baseline selection. This research has shown capability of multi-baseline PolInSAR X-band data for forest parameter estimation while considering the effect of vertical wavenumber k_z on the tree height estimation. A systematic approach of basic SAR data processing, application of both polarimetric and interferometric algorithms are implemented in the height inversion procedure. k_z, is defined by the SAR acquisition geometry and depends on the incidence angle, range and terrain slope. Only a limited range of tree heights can be estimated with a singlek_z. This makes simulation of ideal k_z necessary for the better inversion. Before inversion is performed the non-volumetric decorrelations are minimized by calibration. Temporal decorrelation is a major factor affecting estimation of tree heights from spaceborne data. So, the datasets with temporal baseline of zero days are used.

There are some interesting findings from the results. One major observation is the highly significant improvement in the tree height estimation performance while using a probable baseline to simulate k_z while keeping minimum temporal decorrelation. The calculation of suitable baseline is found to maximize the sensitivity in height estimates. The present work also signifies the importance of the PolInSAR inversion approaches applied. Among the coherence amplitude inversion and three stage inversion, it is concluded that three stage inversion is a robust technique.

In summary, the methodology used in this research can be replicated to allow tree height estimation in any forested area globally. Even if availability of SAR data with optimal baseline over a forest area is limited the tree heights can be estimated with only a prior information about the tallest tree height in a region.

To conclude, the contribution of this research is:

i. Demonstration of the role of vertical wavenumber in the tree height estimation using different inversion techniques.
ii. Development of a methodology to estimate the ideal wavenumber for enhancing the estimation of tree heights.
iii. Demonstration of improvement in tree height estimates with simulated wavenumber for datasets with non-ideal baseline.

7.2. Recommendations

A few recommendations have been listed for future studies:

- The present research observes the effect of wavenumber in X-band dataset only. It is recommended that a similar approach may be adopted for multi-frequency microwave band datasets in further research.
- The present research works with quadratic polarized data. It is recommended that a similar approach may be adopted for single polarization and dual-polarization dataset.
- The proposed technique's capability should further be tested with other datasets and sites. The Barkot-Thano forest area is dominated with mainly homogenous mature Sal Forest. It is suggested that forest types with different stages of maturities and a heterogeneous mixture of species should also be studied using the methodology followed in present research.
- The field data limits the accuracy of the validation process. LIDAR dataset can be used for validation of the estimated tree heights.
- The effect of variation in slope on the estimation of tree heights using simulated baseline can be explored in future studies.
- The impact of changing resolution of the product on the estimation can be explored in future studies.

LIST OF REFERENCES

Bamler, R., & Hartl, P. (1998). Synthetic aperture radar interferometry. *Inverse Problems*, *14*(4), R1–R54. https://doi.org/10.1088/0266-5611/14/4/001

Chen, H., Cloude, S. R., & Goodenough, D. G. (2016). Forest Canopy Height Estimation Using Tandem-X Coherence Data. *IEEE Journal of Selected Topics in Applied Earth Observations and Remote Sensing*, *9*(7), 3177–3188. https://doi.org/10.1109/JSTARS.2016.2582722

Chen, Z., Zhang, L., & Zhang, G. (2016). An improved InSAR image co-registration method for pairs with relatively big distortions or large incoherent areas. *Sensors*, *16*(9). https://doi.org/10.3390/s16091519

Cloude, S. R. (2005). *PoL-InSAR training course. Training Courses for PolSARpro v3.0*. Retrieved from https://earth.esa.int/polsarpro/Manuals/1_Pol-InSAR_Training_Course.pdf

Cloude, S. R. (2010). *Polarisation Applications in Remote Sensing* (1st ed.). New York: Oxford University Press Inc.

Cloude, S. R., Chen, H., & Goodenough, D. G. (2013). Forest height estimation and validation using Tandem-X polinsar. *Proc. International Geoscience and Remote Sensing Symposium (IGARSS)*, 1889–1892. https://doi.org/10.1109/IGARSS.2013.6723172

Cloude, S. R., & Papathanassiou, K. P. (1998). Polarimetric SAR Interferometry. *IEEE Transactions on Geoscience and Remote Sensing*, *36*(5), 1551–1565. https://doi.org/10.1109/36.718859

Cloude, S. R., & Papathanassiou, K. P. (2001). Single-Baseline Polarimetric SAR Interferometry. *IEEE Transactions on Geoscience and Remote Sensing*, *39*(11), 2352–2363. https://doi.org/10.1109/36.964971

Cloude, S. R., & Papathanassiou, K. P. (2003). Three-stage inversion process for polarimetric SAR interferometry. *IEEE Proceedings - Radar, Sonar and Navigation*, *150*(3), 125–134. https://doi.org/10.1049/ip-rsn:20030449

Cloude, S. R., & Pottier, E. (1996). A Review of Target Decomposition Theorems in Radar Polarimetry. *IEEE Transactions on Geoscience and Remote Sensing*, *34*(2), 498–518. https://doi.org/10.1109/36.485127

Dixon, R. K., Brown, S., Houghton, R. E. A., Solomon, A. M., Trexler, M. C., & Wisniewski, J. (1994). Carbon Pools and Flux of Global Forest Ecosystems. *Science*, *263*(5144), 185–190. https://doi.org/10.126/science.263.5144.185

Ferretti, A., Monti-guarnieri, A., Prati, C., & Rocca, F. (2007). *InSAR Principles: Guidelines for SAR Interferometry Processing and Interpretation*. (K. Fletcher, Ed.), *ESA Publications*. https://doi.org/10.1787/9789264101630-5-en

Flynn, T., Tabb, M., & Carande, R. (2002). Coherence Region Shape Extraction for Vegetation Parameter Estimation in Polarimetric SAR Interferometry. *Proceedings of IEEE IGARSS*, 2596–2598. https://doi.org/10.1109/IGARSS.2002.1026712

Fu, H., Zhu, J., Wang, C., Wang, H., & Zhao, R. (2017). Underlying topography estimation over forest areas using high-resolution P-band single-baseline polInSAR data. *Remote Sensing*, *9*(4). https://doi.org/10.3390/rs9040363

Gatelli, F., Guarnieri, A. M., Parizzi, F., Pasquali, P., Prati, C., & Rocca, F. (1994). The Wavenumber Shift in SAR Interferometry. *IEEE Transactions on Geoscience and Remote Sensing*, *32*(4), 855–865. https://doi.org/10.1109/36.298013

Hajnsek, I., Kugler, F., Lee, S., & Papathanassiou, K. P. (2009). Tropical-Forest-Parameter Estimation by Means of Pol-InSAR : The INDREX-II Campaign, *47*(2), 481–493. https://doi.org/10.1109/TGRS.2008.2009437

Hajnsek, I., Papathanassiou, K. P., & Cloude, S. R. (2001). Removal of additive noise in polarimetric eigenvalue processing. *Geoscience and Remote Sensing Symposium, 2001. IGARSS '01. IEEE 2001 International*, *6*(49), 2778–2780 vol.6. https://doi.org/10.1109/igarss.2001.978160

Hellmann, M., & Cloude, S. R. (2007). Polarimetric Interferometry. *Radar Polarimetry and Interferometry*.

Joshi, S. K., Kumar, S., & Agrawal, S. (2016). Performance of PolSAR backscatter and PolInSAR coherence for scattering characterization of forest vegetation using TerraSAR-X data. *Proceedings of SPIE*, *9877*. https://doi.org/10.1117/12.2223898

Krieger, G., Hajnsek, I., Papathanassiou, K. P., Younis, M., & Moreira, A. (2010). Interferometric synthetic aperture radar (SAR) missions employing formation flying. *Proceedings of the IEEE*, *98*(5), 816–843. https://doi.org/10.1109/JPROC.2009.2038948

Krieger, G., Papathanassiou, K. P., & Cloude, S. R. (2005). Spacebourne Polarimetric SAR Interferometry: Performance Analysis and Mission Concepts. *EURASIP Journal on Applied Signal Processing*, *20*, 3272–3292. https://doi.org/10.1155/ASP.2005.3272

Krieger, G., Zink, M., Bachmann, M., Bräutigam, B., Schulze, D., Martone, M., … Moreira, A. (2013). Tandem-X: A Radar Interferometer With Two Formation Flying Satellites. *Acta Astronautica*, *89*, 83–98. https://doi.org/10.1016/j.actaastro.2013.03.008

Kugler, F., Lee, S. K., Hajnsek, I., & Papathanassiou, K. P. (2015). Forest Height Estimation by Means of Pol-InSAR Data Inversion: The Role of the Vertical Wavenumber. *IEEE Transactions on Geoscience and Remote Sensing*, *53*(10), 5294–5311. https://doi.org/10.1109/TGRS.2015.2420996

Kugler, F., Schulze, D., Hajnsek, I., Pretzsch, H., & Papathanassiou, K. P. (2014). TanDEM-X Pol-InSAR Performance for Forest Height Estimation. *IEEE Transactions on Geoscience and Remote Sensing*, *52*(10), 6404–6422. https://doi.org/10.1109/TGRS.2013.2296533

Kumar, S., Dev, R., Kushwaha, G. S. P. S., Jayawardhana, W. G. N. N., & Agarwal, S. (2017). Bistatic PolInSAR Inversion Modelling for Plant Height Retrieval in a Tropical Forest. *Proceedings of the National Academy of Sciences, India Section A: Physical Sciences*, *87*(4), 817–826. https://doi.org/10.1007/s40010-017-0451-9

Kumar, S., Khati, U. G., Chandola, S., Agrawal, S., & Kushwaha, S. P. S. (2017). Polarimetric SAR Interferometry based modeling for tree height and aboveground biomass retrieval in a tropical deciduous forest. *Advances in Space Research*, *60*(3), 571–586. https://doi.org/10.1016/j.asr.2017.04.018

Lavalle, M. (2009). *Full and Compact Polarimetric Radar Interferometry for Vegetation Remote Sensing*. Signal and Image processing. Universit´ e Rennes 1. Retrieved from https://tel.archives-ouvertes.fr/tel-00480972

Le Toan, T., Beaudoin, A., Riom, J., & Guyon, D. (1992). Relating Forest Biomass to SAR Data. *IEEE Transactions on Geoscience and Remote Sensing*, *30*(2), 403–411. https://doi.org/10.1109/36.134089

Lee, S. K. (2012). *Forest Parameter Estimation Using Polarimetric SAR Interferometry Techniques at Low Frequencies*. PhD Thesis, ETH Zurich. https://doi.org/10.3929/ethz-a-007615658

Lee, S. K., Kugler, F., Hajnsek, I., & Papathanassiou, K. P. (2009). The impact of temporal decorrelation over forest terrain in polarimetric SAR interferometry. *European Space Agency, (Special Publication) ESA SP*, *668 SP*.

Lee, S. K., Kugler, F., Papathanassiou, K. P., & Moreira, A. (2009). *K & C Science Report – Phase 1 Forest Height Estimation by means of Pol-InSAR Limitations posed by Temporal Decorrelation*. Tsukuba, Japan.

Lin, D., Zhu, J., Fu, H., Xie, Q., & Zhang, B. (2017). A TSVD-Based Method for Forest Height Inversion from Single-Baseline PolInSAR Data. *Applied Sciences*, *7*(5), 435. https://doi.org/10.3390/app7050435

Lopez-Sanchez, J. M., Vicente-Guijalba, F., Erten, E., Campos-Taberner, M., & Garcia-Haro, F. J. (2017). Retrieval of vegetation height in rice fields using polarimetric SAR interferometry with TanDEM-X data. *Remote Sensing of Environment*, *192*, 30–44. https://doi.org/10.1016/j.rse.2017.02.004

Neumann, M., Ferro-Famil, L., & Reigber, A. (2008). Multibaseline polarimetric SAR interferometry coherence optimization. *IEEE Geoscience and Remote Sensing Letters*, *5*(1), 93–97. https://doi.org/10.1109/LGRS.2007.908885

Neumann, M., Ferro-Famil, L., & Reigber, A. (2010). Estimation of forest structure, ground, and canopy layer characteristics from multibaseline polarimetric interferometric SAR data. *IEEE Transactions on Geoscience and Remote Sensing*, *48*(3), 1086–1104. https://doi.org/10.1109/TGRS.2009.2031101

Olesk, A., Praks, J., Antropov, O., Zalite, K., Arumäe, T., & Voormansik, K. (2016). Interferometric SAR coherence models for Characterization of hemiboreal forests using TanDEM-X data. *Remote Sensing*, *8*(9). https://doi.org/10.3390/rs8090700

Perko, R., Raggam, H., Deutscher, J., Gutjahr, K., & Schardt, M. (2011). Forest assessment using high resolution SAR data in X-Band. *Remote Sensing*, *3*(4), 792–815. https://doi.org/10.3390/rs3040792

Praks, J., Hallikainen, M., Seppänen, J., & Hyyppä, J. (2009). Boreal forest height estimation with SAR interferometry and laser measurements. *International Geoscience and Remote Sensing Symposium (IGARSS)*, *5*, 308–311, July 2009. https://doi.org/10.1109/IGARSS.2009.5417669

Ranson, K. J., Sun, G., Weishampel, J. F., & Knox, B. G. (1997). Forest Radar Biomass from combined Backscatter Modeling. *Remote Sensing of Environment*, *59*(96), 118–133. https://doi.org/10.1016/S0034-4257(96)00114-9

Sagués, L., Lopez-Sanchez, J. M., Fortuny, J., Fàbregas, X., Broquetas, A., & Sieber, A. J. (2000). Indoor experiments on polarimetric SAR interferometry. *IEEE Transactions on Geoscience and Remote Sensing*, *38*(2), 671–684. https://doi.org/10.1109/36.841997

Singh, S. P. (2010). Impact of Forest Degradation on Carbon Density in Soil and Vegetation of. *International Journal of Climatology*, *23*(5), 693–705. https://doi.org/10.1016/j.rse.2009.12.014

Tebaldini, S. (2012). Forest structure retrieval from multi-baseline SARs. *Remote Sensing of Biomass - Principles and Applications* (pp. 27–58). (L. Fatoyinbo Ed.). InTech. https://doi.org/10.5772/696

Tong, H., Dinh, M., Toan, T. Le, Rocca, F., Tebaldini, S., Villard, L., & Réjou-méchain, M. (2016). SAR tomography for the retrieval of forest biomass and height : Results from two tropical forests in French Guiana. *Remote Sens. Environ.*, *175*, 138–147. https://doi.org/10.1016/j.rse.2015.12.037

Touzi, R., Lopes, A., Bruniquel, J., & Vachon, P. W. (1999). Coherence estimation for SAR imagery. *IEEE Transactions on Geoscience and Remote Sensing*, *37*(1), 135–149. https://doi.org/10.1109/36.739146

Treuhaft, R. N., & Siqueira, P. R. (2000). Vertical structure of vegetated land surfaces from interferometric and polarimetric radar. *Radio Science*, *35*(1), 141–177.

van Der Sanden, J. J. (1997). *Radar Remote Sensing To Support Tropical Forest Management. Tropenbos-Guyana Series 5*. PhD Thesis, Wageningen Agricultural University. Retrieved from http://www.tropenbos.org/publications/radar+remote+sensing+to+support+tropical+forest+management+-++tropenbos+guyana+series+5

Vashum, K. T., & Jayakumar, S. (2012). Ecosystem & Ecography Methods to Estimate Above-Ground Biomass and Carbon Stock in Natural Forests - A Review. *J Ecosyst Ecogr*, *2:116*(4). https://doi.org/10.4172/2157-7625.1000116

Yamada, H., Yamaguchi, Y., Rodriguez, E., Kim, Y., & Boerner, W. M. (2001). Polarimetric SAR interferometry for forest canopy analysis by using the super-resolution method. In *IGARSS 2001. Scanning the Present and Resolving the Future. Proceedings. IEEE 2001 International Geoscience and Remote Sensing Symposium (Cat. No.01CH37217)* (Vol. 3, pp. 7031–7033). https://doi.org/10.1109/IGARSS.2001.976759

Zebker, H. A., & Villasenor, J. (1992). Decorrelation in Inteferometric Radar Echoes. *IEEE Transactions on Geoscience and Remote Sensing*, *30*(5), 950–959.

Zhang, L., Duan, B., & Zou, B. (2017). Research on Inversion Models for Forest Height Estimation Using Polarimetric SAR Interferometry. *ISPRS - International Archives of the Photogrammetry, Remote Sensing and Spatial Information Sciences*, *XLII*(September), 659–663. https://doi.org/10.5194/isprs-archives-XLII-2-W7-659-2017

Zhou, Z. B., Ma, H. Z., Zhu, X. B., & Sun, L. (2013). Comparative Analysis of Forest Height Retrieval Methods by Polarimetric SAR Interferometry. *Advanced Materials Research*, *726–731*(1), 4686–4689. https://doi.org/10.4028/www.scientific.net/AMR.726-731.4686

APPENDIX 1: SAR BASICS

A radar system works on the transmission and reception of electromagnetic signals. Electromagnetic waves travelling from the transmitter to the target and back undergo change in polarization depending on the type of target. The single look complex image is obtained in slant range geometry which represents the distance of the target from the radar. The objects towards the near range are compressed as compared to the object in the far range. Multi-looking converts the slant range into ground range by making azimuth and range resolutions equal. PolSAR techniques allow the differentiation of various scattering mechanisms and their decomposition to identify the scatterers. Polarization permits the measurement of target information. A fully polarimetric system implements both horizontal and vertical polarizations with four polarization channels, two co-polarized channels HH and VV and two cross-polarized channels HV and VH. The scattering matrix $[S]$ stores the values measured in these polarization channels and provides the relationship between the incident and scattered electromagnetic wave given as:

$$[S] = \begin{bmatrix} S_{HH} & S_{HV} \\ S_{VH} & S_{VV} \end{bmatrix} \quad \text{(A1.1)}$$

The scattering matrix contains the pixel wise information of amplitude and phase of the signals. Complex targets like vegetation are analysed using coherency matrix formed with the scattering information given as:

$$\begin{bmatrix} <|S_{HH}+S_{VV}|^2> & <(S_{HH}+S_{VV})(S_{HH}-S_{VV})^*> & 2<(S_{HH}+S_{VV})S_{HV}^*> \\ <(S_{HH}-S_{VV})(S_{HH}+S_{VV})^*> & <|S_{HH}-S_{VV}|^2> & 2<(S_{HH}-S_{VV})S_{HV}^*> \\ 2<S_{HV}(S_{HH}+S_{VV})^*> & 2<S_{HV}(S_{HH}-S_{VV})^*> & 4<|S_{HV}|^2> \end{bmatrix} \quad \text{(A1.2)}$$

The decomposition of coherency matrix identifies different scattering mechanisms as surface, double-bounce and volume scattering. Complex scattering medium like forests have various scatterers present under the canopy. The scattering mechanisms can be interpreted by PolInSAR as the physical properties of scatterers are related to the features observed. Both polarimetric and interferometric information and their combination is implemented in Polarimetric SAR Interferometry (PolInSAR).

APPENDIX 2: EFFECT OF TOPOGRAPHIC VARIATION ON WAVENUMBER

The terrain slope α is an important factor which influences the local incidence angle crucial for the calculation of vertical wavenumber. The slope only in range direction is considered useful while the slope in azimuth direction is considered insignificant. The slope affects the $k_z$as:

$$k_z = m\frac{2\pi}{\lambda}\frac{B_\perp}{R\sin(\theta+\alpha)} \tag{A2.1}$$

When the terrain slope is slanted towards the satellite the local incidence angle is decreased by α and when the terrain slope is slanted away from the satellite the local incidence angle is increased by α. When the terrain is inclined towards the satellite the $k_z$will increase and when the terrain is inclined away from the satellite the k_z decreases.

The forest height estimateH_f, for sloped topography, is given as:

$$H_f = \frac{h_v}{\cos|\alpha|} \tag{A2.2}$$

where h_v is the perpendicular height. The correct estimation of the αdepends on the accuracy of the DEM used. In this research SRTM DEM is used to evaluate the slope in the study area. The difference in slope in the range direction is calculated to find the variability of elevation in the study area (FigureA29). In the scene, pixels have elevation difference ranging between -2.5 to +2.5 m,α values as less than 1.80e-06 and cos|α| values less than 1 from which it is established that the forest height in this region is not affected by the topography and its effect can be kept apart from this study.

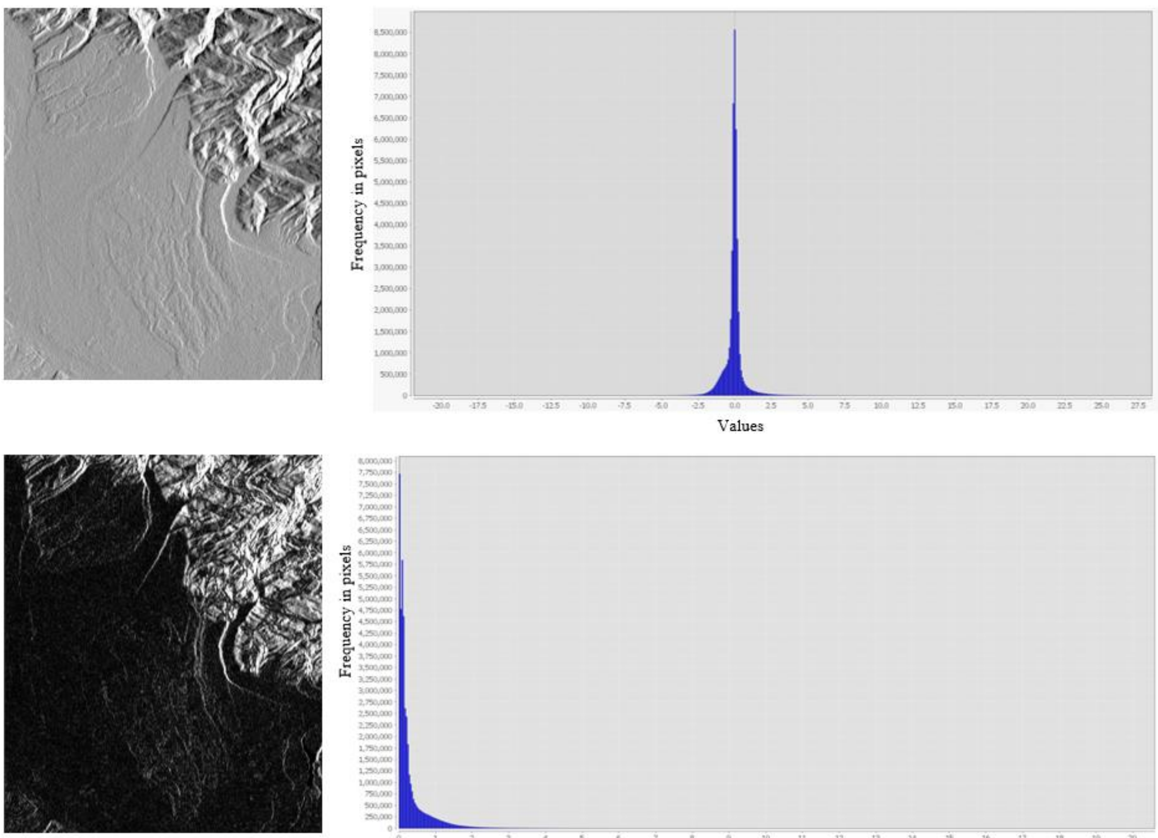

Figure A29. Top: Elevation difference in the range direction with the frequency plot of elevation difference. Bottom: cos|α| image and frequency plot

APPENDIX 3: INVERSION BASED MODELLED OUTPUT

The forest height estimates for coherence amplitude inversion and three-stage inversion with simulated wavenumber ($k_z = 0.21$) are shown in Figure A30 and Figure A31.

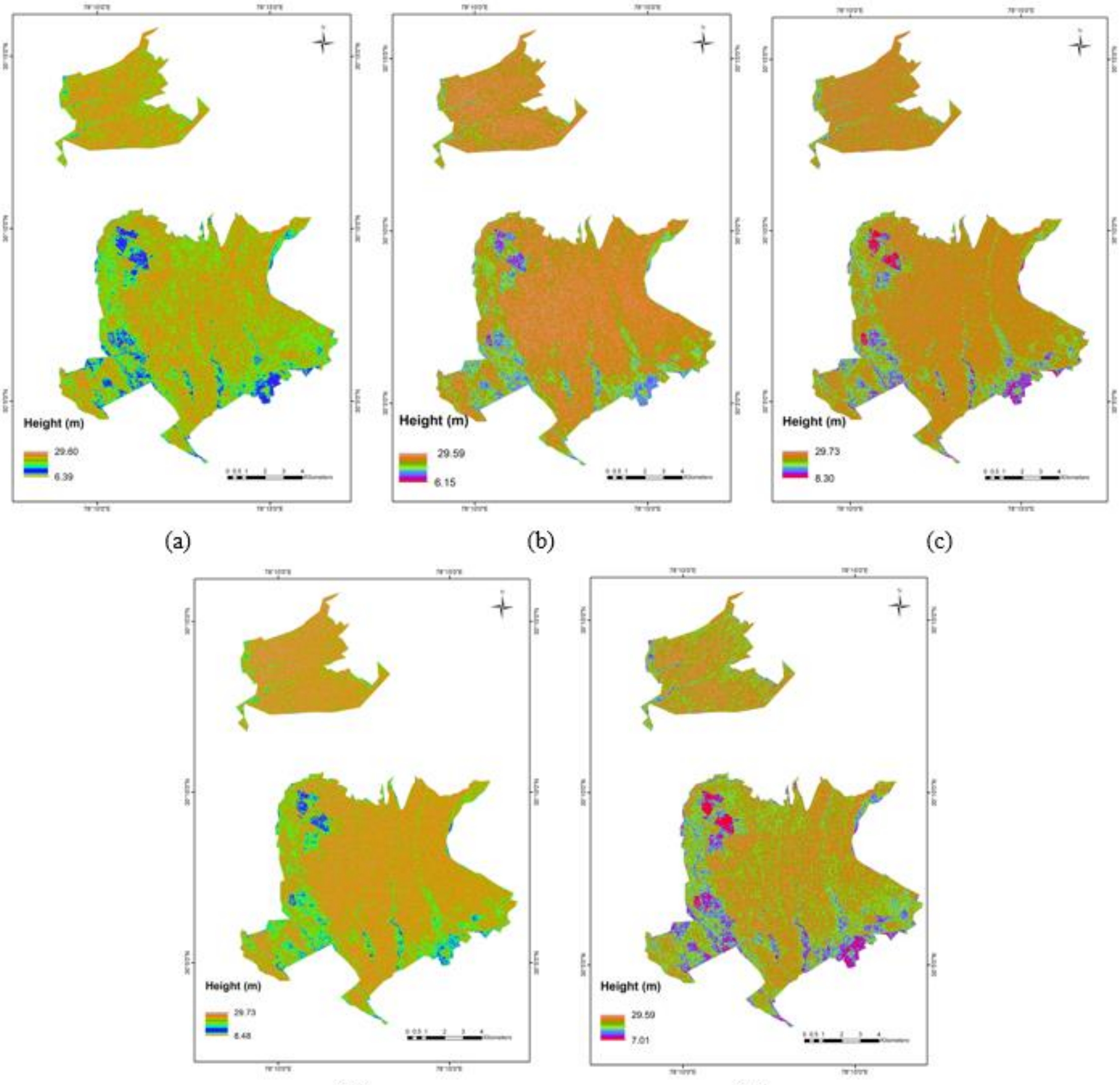

Figure A30. Coherence amplitude inversion based modelled output (a) 19th December 2014 (b) 21st January 2015 (c) 1st February 2015 (d) 12th February 2015 (e) 23rd February 2015

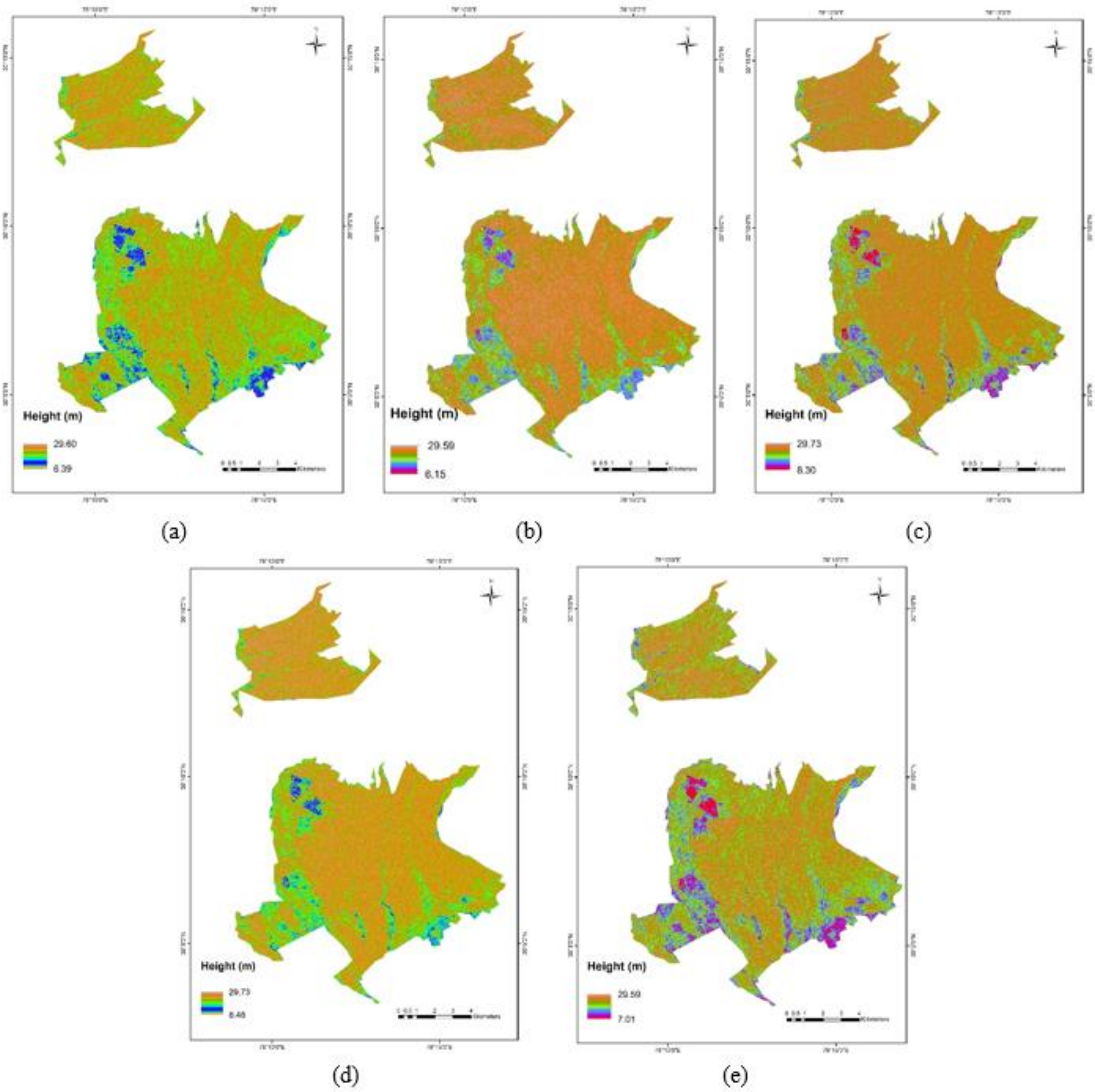

Figure A31. Three-stage inversion based modelled output (a) 19th December 2014 (b) 21st January 2015 (c) 1st February 2015 (d) 12th February 2015 (e) 23rd February 2015